Table 4
Predictive factors for transmission of drug-resistant HIV-1.

	Drug-resistant HIV-1 (*n*)		Odds ratio
	(+)	(−)	
Gender			
Male	183	2214	1.92
Female	7	163	
Nationality			
Japanese	173	2146	1.05
Non-Japanese	16	209	
Transmission category			
Male-to-male sexual contact	130	1643	0.91
High-risk heterosexual contact	37	484	
Sexual contact	15	60	
Other	1	40	
Unidentified[a]	11	152	
Subtype			
B	180	2014	2.36*
Non-B	11	291	
Unidentified	3	77	

[a] For calculation of odds ratio, unidentified cases were omitted.
* $p < 0.01$.

tions that were detected only sporadically throughout the study period (supplementary Table 2).

Analysis of possible predictive factors for transmission of drug-resistant HIV-1 showed that individuals infected with subtype B HIV-1 had a significantly higher tendency to harbor drug-resistant HIV-1 than non-B subtypes (OR = 2.36; 95% CI = 1.27–4.88; $p < 0.01$) (Table 4). Other possible predictive factors, including male gender (OR = 1.92; 95% CI = 0.89–4.93; $p = 0.1$), Japanese nationality (OR = 1.05; 95% CI = 0.62–1.92; $p = 1$), and MSM behavior (OR = 0.91; 95% CI 0.66–1.26; $p = 0.57$), were not significant predictive factors in our study population. These results indicate that the chance of getting infected with drug-resistant HIV-1 was the same for anyone regardless of gender, nationality, or risk behavior.

3.4. MSM are diagnosed earlier than heterosexually infected individuals

To examine awareness of HIV infection, especially of risk behavior, and to characterize HIV-testing patterns among the HIV-infected population, we estimated the time of seroconversion by quantifying the amount of anti-HIV antibody in plasma samples. Of 640 randomly selected samples in 2007 and 2008, 233 (36.4%) were classified by BED assay with a cut-off value of 0.8 as recently infected (<155-day seroconversion), while the remaining 407 (63.4%) were classified as not recently infected (Table 5). For the recently and not recently infected groups, the average $CD4^+$ T cell count and HIV-1 viral load were 285 and 215 cells/μL and 5.1×10^5 and 1.4×10^5 copies/mL, respectively. Recently infected individuals were shown by ANCOVA with $CD4^+$ T cell counts as the covariate, to have significantly higher HIV-1 viral loads than not recently infected cases (Fig. 2). These data support that the BED assay had precisely determined early infected cases.

With respect to risk behavior, the highest rate of recent infection was in MSM (39.2%), followed by either homo- or heterosexual contacts (38.9%), and heterosexual contacts (25.0%). No patients infected through a risk behavior other than sexual contacts were categorized as recently infected. Whereas 37.8% of male patients were determined to be recently infected, only 13.8% of female patients were categorized as recently infected. These findings were reinforced by statistical analysis. Recent HIV-1 infection was significantly predicted by male gender (OR = 3.79; 95% CI 1.29–15.17; $p < 0.01$), MSM behavior (OR = 1.67; 95% CI = 1.11–2.54; $p = 0.01$), Japanese nationality (OR = 2.31; 95% CI 1.20–4.76; $p < 0.01$), and infection with subtype B HIV-1 (OR = 5.64; 95% CI = 2.37–16.33; $p < 0.01$) (Table 5). In other words, Japanese males, especially those who were MSM, were more aware of being at high risk of HIV-1 infection and got tested more often than non-Japanese. In contrast, females, individuals of non-Japanese origin, heterosexuals, and non-subtype-B-infected persons, had low awareness of the risks of HIV-1 infection.

Table 5
Predictive factors for recent or not-recent seroconversion determined by BED assay, $n = 640$.

	Seroconversion (*n*)		Odds ratio
	Recent ($n = 233$)	Not recent ($n = 407$)	
Gender			
Male	229	377	3.79*
Female	4	25	
Unknown[b]	0	5	
Nationality			
Japanese	220	351	2.31*
Non-Japanese	13	48	
Unknown[b]	0	8	
Transmission category			
Male-to-male sexual contact	189	293	1.67[a,*]
High-risk heterosexual contact	24	70	
Sexual contact	7	11	
Other	0	4	
Unidentified[b]	13	29	
Subtype			
B	224	350	5.64*
Non-B	6	53	
Unidentified[b]	3	4	
Drug-resistant HIV			
Detected	14	37	0.64
Not detected	219	370	

[a] Odds ratio for the transmission category was calculated between male-to-male sexual contact and other categories which include high-risk heterosexual contact, sexual contact, and other.
[b] Unknown or unidentified cases were omitted in calculation of odds ratio.
† $p < 0.05$.
* $p < 0.01$.

Regarding associations between the time of diagnosis and drug-resistant HIV transmission event, time of diagnosis did not differ significantly between those harboring and those not harboring drug-resistant HIV-1 (OR = 0.64; 95% CI = 0.31–1.24; $p = 0.18$) (Table 5), suggesting that transmission of drug-resistant HIV-1 is not a recent trend, but has been ongoing since the first antiretroviral, AZT, was introduced in 1986.

4. Discussion

Our study results show that the proportion of drug-resistant HIV-1 among newly diagnosed cases in Japan increased slightly (by 2.4%) from 2003 to 2008, with fluctuations from year to year. Drug-resistant HIV-1 in HAART-naïve patients are transmitted from HAART-experienced patients with inadequate adherence or from other treatment-naïve individuals with drug-resistant strains, but not yet diagnosed or tested for drug-resistant HIV-1 (de Mendoza et al., 2005). Hence, drug-resistant mutations detected in the naïve population should be tightly related to trends in antiretroviral use in the treated population. Antiretrovirals available in the early days of the HAART era, especially, had short half-lives and low genetic barriers for drug resistance acquisition, making the viruses easily resistance prone. On the other hand, new antiretroviral drugs, such as lopinavir, atazanavir, amprenavir and darunavir, have been developed so that they have improved pharmacokinetics and higher genetic barriers, thus the viruses have less chance of developing drug resistance (Dunn et al., 2008; Lima et al., 2008; Zajdenverg et al., 2009). In the present study, we found that drug-resistant mutations detected among treatment-naïve patients were

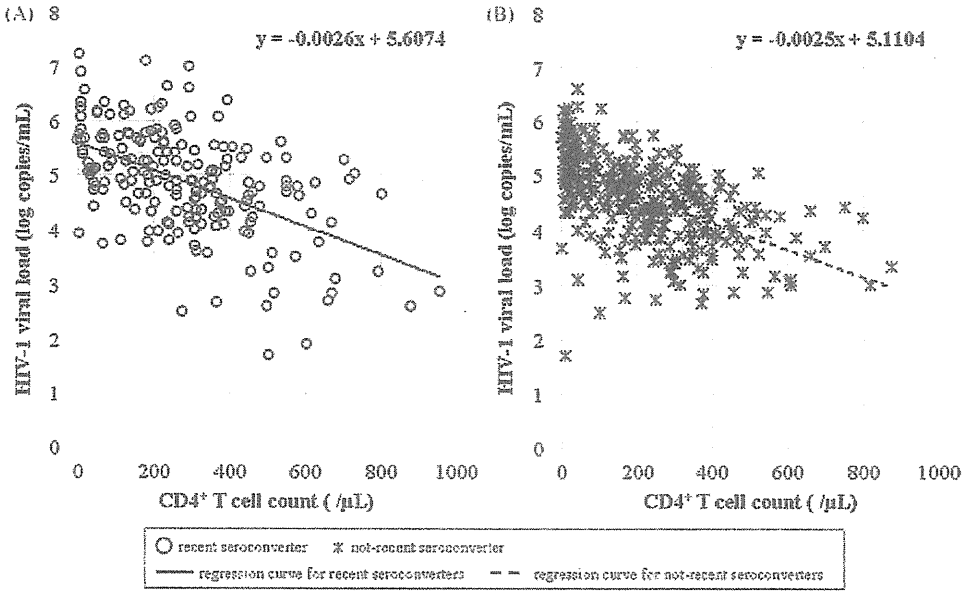

Fig. 2. Scatter plots of viral load and CD4+ T cell counts for (A) recently seroconverted patients ( ), and (B) not recently seroconverted patients ( ) determined by BED assay. Regression curves and their equations are shown for each group.

associated especially with antiretrovirals used prior to and early in the HAART era. It should be noted that contrary to the reports from the United States and many of European countries (Audelin et al., 2009; Vercauteren et al., 2009; Wheeler et al., 2010), the prevalence of NNRTI-resistant variants have been determined to be low in Japan, less than 1% in the study period 2003–2007 and 1.3% in 2008 being the highest. This difference is due to the situation in Japan that delavirdine had never been used and even nevirapine is only rarely prescribed. Nonetheless, strains with T215X, M46I/L, K103N, and M184V/I mutations were detected every year, suggesting that these strains are stably maintained in individuals and in high-risk populations even under antiretroviral drug-free environments. This finding is supported by the insignificant difference in prevalence of drug-resistant HIV-1 between recently and not recently infected groups. These results raise the concern that such drug-resistant strains may have become some epidemic strains actively transmitted among newly diagnosed HIV/AIDS patients. Furthermore, considering the presence of low frequent variants, the prevalence of drug-resistant mutations in this report may be higher if more sensitive techniques, such as allele-specific PCR and ultra-deep sequencing, are applied to test the samples (Halvas et al., 2010; Varghese et al., 2009). Further studies employing such techniques are needed to understand the detailed epidemic in Japan.

In investigating predictive factors for transmission of drug-resistant strains, we found that the only predictive factor was subtype B HIV-1 (OR = 2.36, $p < 0.01$). The lower transmission risk of drug-resistant strains in non-B HIV-1 can be explained by patients' countries of origin. We observed a significant relationship between non-B subtype HIV-1 and non-Japanese patients, most of whom were from developing countries with limited access to antiretrovirals. Thus, our finding agrees with reports of low prevalence drug-resistant HIV-1 transmission in developing countries (Bártolo et al., 2009; Ishizaki et al., 2009; Mintsa-Ndong et al., 2009; Ndembi et al., 2008; Nouhin et al., 2009; Pillay et al., 2008).

Interestingly, a high proportion of Japanese MSM was diagnosed as recently infected compared to patients of non-Japanese origin, and females determined by BED assay. This result may be due to successful prevention programs targeting the MSM community, so that they have become more aware of their risks of HIV-1 infection. On the other hand, many of non-Japanese patients are seen at hospitals long after HIV infection is established. In addition, women tend to be ignorant of the risks of HIV infection, thus they are often diagnosed upon a prenatal HIV screening test.

Although MSM was not a predictive factor for transmission, this group included 130 cases with drug-resistant HIV-1, the highest prevalence among all the transmission categories. Therefore, those who are involved in prevention programs should take one step further to remind the MSM community about drug-resistant HIV-1 and the limited choice of effective antiretrovirals. HIV-1 transmission has been reported to be prevented in models that assessed the effect of HIV-1 testing for wider populations and immediate initiation of antiretroviral therapy (Granich et al., 2009). Although this model seems very appealing, our results suggest the importance of not forgetting the emergence and transmission of drug-resistant HIV-1 and the limited selection of antiretroviral drugs. It is important to continue surveying newly diagnosed HIV/AIDS patients to keep track of trends in drug-resistant HIV-1 transmission, to reveal high-risk populations with low awareness of HIV infection, to propose effective programs to prevent transmission of drug-resistant HIV-1, and to develop antiretroviral drugs with improved pharmacokinetics/pharmacodynamics. All these efforts may bring us one step closer to eradicating HIV-1.

Acknowledgments

We are grateful to all the patients who participated in our surveillance study. We thank the members of Japanese Drug Resistance HIV-1 Surveillance Network for their support and helpful discussions: Atsushi Ajisawa, Hitoshi Chiba, Takeshi Fujii, Yuko Fujikawa, Akira Fujita, Katsuyuki Fukutake, Tetsushi Goto, Shuji Hatakeyama, Igen Hongo, Masahide Horiba, Mitsunobu Imai, Tsuguhiro Kaneda, Akiro Kimura, Mitsuru Konishi, Shuzo Matsushita, Motoo Matsuura, Naoko Miyazaki, Itsuhiro Nakagiri, Masaaki Noda, Tsuyoshi Oishi, Chiho Otani, Takeyuki Sato, Satoshi Shirahata, Masashi Taki, Sadahiro Tamashima, Masanori Tei, Kazue Uchida,

Kanako Watanabe, Yasuyuki Yamamoto, Kunio Yano, Mihoko Yotsumoto. We also thank Claire Baldwin for her help in preparing the manuscript. This study was supported by a Grant-in-Aid for AIDS research from the Ministry of Health, Labour, and Welfare of Japan (H19-AIDS-007). The sponsor had no role in study design, data collection and analysis, decision to publish, or preparation of the manuscript.

Appendix A. Supplementary data

Supplementary data associated with this article can be found, in the online version, at doi:10.1016/j.antiviral.2010.07.008.

References

Apisarnthanarak, A., Jirayasethpong, T., Sa-nguansilp, C., Thongprapai, H., Kittihanukul, C., Kamudamas, A., Tungsathapornpong, A., Mundy, L.M., 2008. Antiretroviral drug resistance among antiretroviral-naive persons with recent HIV infection in Thailand. HIV Med. 9, 322–325.

Audelin, A.M., Lohse, N., Obel, N., Gerstoft, J., Jørgensen, L.B., 2009. The incidence rate of HIV type-1 drug resistance in patients on antiretroviral therapy: a nationwide population-based Danish cohort study 1999–2005. Antivir. Ther. 14, 995–1000.

Bártolo, I., Rocha, C., Bartolomeu, J., Gama, A., Fonseca, M., Mendes, A., Cristina, F., Thamm, S., Epalanga, M., Silva, P.C., Taveira, N., 2009. Antiretroviral drug resistance surveillance among treatment-naive human immunodeficiency virus type 1-infected individuals in Angola: evidence for low level of transmitted drug resistance. Antimicrob. Agents Chemother. 53, 3156–3158.

Bennett, D.E., Camacho, R.J., Otelea, D., Kuritzkes, D.R., Fleury, H., Kiuchi, M., Heneine, W., Kantor, R., Jordan, M.R., Schapiro, J.M., Vandamme, A.M., Sandstrom, P., Boucher, C.A., van de Vijver, D., Rhee, S.Y., Liu, T.F., Pillay, D., Shafer, R.W., 2009. Drug resistance mutations for surveillance of transmitted HIV-1 drug-resistance: 2009 update. PLoS One 4, e4724.

Boden, D., Hurley, A., Zhang, L., Cao, Y., Guo, Y., Jones, E., Tsay, J., Ip, J., Farthing, C., Limoli, K., Parkin, N., Markowitz, M., 1999. HIV-1 drug resistance in newly infected individuals. JAMA 282, 1135–1141.

Chaix, M.L., Descamps, D., Wirden, M., Bocket, L., Delaugerre, C., Tamalet, C., Schneider, V., Izopet, J., Masquelier, B., Rouzioux, C., Meyer, L., Costagliola, D., 2009. Stable frequency of HIV-1 transmitted drug resistance in patients at the time of primary infection over 1996–2006 in France. AIDS 23, 717–724.

Chang, S.Y., Chen, M.Y., Lee, C.N., Sun, H.Y., Ko, W., Chang, S.F., Chang, K.L., Hsieh, S.M., Sheng, W.H., Liu, W.C., Wu, C.H., Kao, C.L., Hung, C.C., Chang, S.C., 2008. Trends of antiretroviral drug resistance in treatment-naive patients with human immunodeficiency virus type 1 infection in Taiwan. J. Antimicrob. Chemother. 61, 689–693.

de Mendoza, C., Rodriguez, C., Eiros, J.M., Colomina, J., Garcia, F., Leiva, P., Torre-Cisneros, J., Aguero, J., Pedreira, J., Viciana, I., Corral, A., del Romero, J., Ortiz de Lejarazu, R., Soriano, V., 2005. Antiretroviral recommendations may influence the rate of transmission of drug-resistant HIV type 1. Clin. Infect. Dis. 41, 227–232.

DHHS, 2009. Panel on antiretroviral guidelines for adults and adolescents. Guidelines for the use of antiretroviral agents in HIV-1-infected adults and adolescents.

Dunn, D., Geretti, A.M., Green, H., Fearnhill, E., Pozniak, A., Churchill, D., Pillay, D., Sabin, C., Phillips, A., 2008. Population trends in the prevalence and patterns of protease resistance related to exposure to unboosted and boosted protease inhibitors. Antivir. Ther. 13, 771–777.

Eshleman, S.H., Husnik, M., Hudelson, S., Donnell, D., Huang, Y., Huang, W., Hart, S., Jackson, B., Coates, T., Chesney, M., Koblin, B., 2007. Antiretroviral drug resistance, HIV-1 tropism, and HIV-1 subtype among men who have sex with men with recent HIV-1 infection. AIDS 21, 1165–1174.

Fujisaki, S., Fujisaki, S., Ibe, S., Asagi, T., Itoh, T., Yoshida, S., Koike, T., Oie, M., Konda, M., Sadamasu, K., Nagashima, M., Gatanaga, H., Matsuda, M., Ueda, M., Masakane, A., Hata, M., Mizogami, Y., Mori, H., Minami, R., Okada, K., Watanabe, K., Shirasaka, T., Oka, S., Sugiura, W., Kaneda, T., 2007. Performance and quality assurance of genotypic drug-resistance testing for human immunodeficiency virus type 1 in Japan. Jpn. J. Infect. Dis. 60, 113–117.

Gallego, O., Ruiz, L., Vallejo, A., Ferrer, E., Rubio, A., Clotet, B., Leal, M., Soriano, V., 2001. Changes in the rate of genotypic resistance to antiretroviral drugs in Spain. AIDS 15, 1894–1896.

Gatanaga, H., Ibe, S., Matsuda, M., Yoshida, S., Asagi, T., Kondo, M., Sadamasu, K., Tsukada, H., Masakane, A., Mori, H., Takata, N., Minami, R., Tateyama, M., Koike, T., Itoh, T., Imai, M., Nagashima, M., Gejyo, F., Ueda, M., Hamaguchi, M., Kojima, Y., Shirasaka, T., Kimura, A., Yamamoto, M., Fujita, J., Oka, S., Sugiura, W., 2007. Drug-resistant HIV-1 prevalence in patients newly diagnosed with HIV/AIDS in Japan. Antiviral Res. 75, 75–82.

Gómez-Cano, M., Rubio, A., Puig, T., Pérez-Olmeda, M., Ruiz, L., Soriano, V., Pineda, J.A., Zamora, L., Xaus, N., Clotet, B., Leal, M., 1998. Prevalence of genotypic resistance to nucleoside analogues in antiretroviral-naive and antiretroviral-experienced HIV-infected patients in Spain. AIDS 12, 1015–1020.

Granich, R.M., Gilks, C.F., Dye, C., De Cock, K.M., Williams, B.G., 2009. Universal voluntary HIV testing with immediate antiretroviral therapy as a strategy for elimination of HIV transmission: a mathematical model. Lancet 373, 48–57.

Halvas, E.K., Wiegand, A., Boltz, V.F., Kearney, M., Nissley, D., Wantman, M., Hammer, S.M., Palmer, S., Vaida, F., Coffin, J.M., Mellors, J.W., 2010. Low frequency nonnucleoside reverse-transcriptase inhibitor-resistant variants contribute to failure of efavirenz-containing regimens in treatment-experienced patients. J. Infect. Dis. 201, 672–680.

Hirsch, M.S., Brun-Vézinet, F., D'Aquila, R.T., Hammer, S.M., Johnson, V.A., Kuritzkes, D.R., Loveday, C., Mellors, J.W., Clotet, B., Conway, B., Demeter, L.M., Vella, S., Jacobsen, D.M., Richman, D.D., 2000. Antiretroviral drug resistance testing in adult HIV-1 infection: recommendations of an International AIDS Society-USA Panel. JAMA 283, 2417–2426.

Hirsch, M.S., Günthard, H.F., Schapiro, J.M., Brun-Vézinet, F., Clotet, B., Hammer, S.M., Johnson, V.A., Kuritzkes, D.R., Mellors, J.W., Pillay, D., Yeni, P.G., Jacobsen, D.M., Richman, D.D., 2008. Antiretroviral drug resistance testing in adult HIV-1 infection: 2008 recommendations of an International AIDS Society-USA panel. Clin. Infect. Dis. 47, 266–285.

Ishizaki, A., Cuong, N.H., Thuc, P.V., Trung, N.V., Saijoh, K., Kageyama, S., Ishigaki, K., Tanuma, J., Oka, S., Ichimura, H., 2009. Profile of HIV type 1 infection and genotypic resistance mutations to antiretroviral drugs in treatment-naive HIV type 1-infected individuals in Hai Phong, Viet Nam. AIDS Res. Hum. Retroviruses 25, 175–182.

Lall, M., Gupta, R.M., Sen, S., Kapila, K., Tripathy, S.P., Paranjape, R.S., 2008. Profile of primary resistance in HIV-1-infected treatment-naive individuals from Western India. AIDS Res. Hum. Retroviruses 24, 987–990.

Lima, V.D., Gill, V.S., Yip, B., Hogg, R.S., Montaner, J.S., Harrigan, P.R., 2008. Increased resilience to the development of drug resistance with modern boosted protease inhibitor-based highly active antiretroviral therapy. J. Infect. Dis. 198, 51–58.

Los-Alamos, 2010. HIV Databases, http://www.hiv.lanl.gov/content/index.

Maia Teixeira, S.L., Bastos, F.I., Hacker, M.A., Guimarães, M.L., Morgado, M.G., 2006. Trends in drug resistance mutations in antiretroviral-naïve intravenous drug users of Rio de Janeiro. J. Med. Virol. 78, 764–769.

Mintsa-Ndong, A., Caron, M., Plantier, J.C., Makuwa, M., Le Hello, S., Courgnaud, V., Roques, P., Kazanji, M., 2009. High HIV Type 1 prevalence and wide genetic diversity with dominance of recombinant strains but low level of antiretroviral drug-resistance mutations in untreated patients in northeast Gabon, Central Africa. AIDS Res. Hum. Retroviruses 25, 411–418.

Ndembi, N., Lyagoba, F., Nanteza, B., Kushemererwa, G., Serwanga, J., Katongole-Mbidde, E., Grosskurth, H., Kaleebu, P., 2008. Transmitted antiretroviral drug resistance surveillance among newly HIV type 1-diagnosed women attending an antenatal clinic in Entebbe Uganda. AIDS Res. Hum. Retroviruses 24, 889–895.

Nouhin, J., Ngin, S., Martin, P.R., Marcy, O., Kruy, L., Ariey, F., Peeters, M., Chaix, M.L., Ayouba, A., Nerrienet, E., 2009. Low prevalence of drug resistance transmitted virus in HIV Type 1-infected ARV-naive patients in Cambodia. AIDS Res. Hum. Retroviruses 25, 543–545.

Ockenga, J., Tillmann, H.L., Trautwein, C., Stoll, M., Manns, M.P., Schmidt, R.E., 1997. Hepatitis B and C in HIV-infected patients. Prevalence and prognostic value. J. Hepatol. 27, 18–24.

Palma, A.C., Araújo, F., Duque, V., Borges, F., Paixão, M.T., Camacho, R., 2007. Molecular epidemiology and prevalence of drug resistance-associated mutations in newly diagnosed HIV-1 patients in Portugal. Infect. Genet. Evol. 7, 391–398.

Pillay, V., Ledwaba, J., Hunt, G., Rakgotho, M., Singh, B., Makubalo, L., Bennett, D.E., Puren, A., Morris, L., 2008. Antiretroviral drug resistance surveillance among drug-naive HIV-1-infected individuals in Gauteng Province, South Africa in 2002 and 2004. Antivir. Ther. 13 (Suppl. (2)), 101–107.

Piroth, L., Grappin, M., Cuzin, L., Mouton, Y., Bouchard, O., Raffi, F., Rey, D., Peyramond, D., Gourdon, F., Drobacheff, C., Lombart, M.L., Lucht, F., Besnier, J.M., Bernard, L., Chavanet, P., Portier, H., 2000. Hepatitis C virus co-infection is a negative prognostic factor for clinical evolution in human immunodeficiency virus-positive patients. J. Viral Hepat. 7, 302–308.

Sagir, A., Oette, M., Kaiser, R., Däumer, M., Fätkenheuer, G., Rockstroh, J.K., Knechten, H., Schmutz, G., Hower, M., Emmelkamp, J., Pfister, H., Haussinger, D., 2007. Trends of prevalence of primary HIV drug resistance in Germany. J. Antimicrob. Chemother. 60, 843–848.

Tambussi, G., Boeri, E., Carrera, P., Gianotti, N., Lazzarin, A., 1998. Prevalence of mutation associated to resistance with nucleoside analogues in a cohort of naïve HIV-1 positive subjects during the period 1984–1997. J. Biol. Regul. Homeost. Agents 12, 32–34.

Varghese, V., Shahriar, R., Rhee, S.Y., Liu, T., Simen, B.B., Egholm, M., Hanczaruk, B., Blake, L.A., Gharizadeh, B., Babrzadeh, F., Bachmann, M.H., Fessel, W.J., Shafer, R.W., 2009. Minority variants associated with transmitted and acquired HIV-1 nonnucleoside reverse transcriptase inhibitor resistance: implications for the use of second-generation nonnucleoside reverse transcriptase inhibitors. J. Acquir. Immune Defic. Syndr. 52, 309–315.

Vercauteren, J., Derdelinckx, I., Sasse, A., Bogaert, M., Ceunen, H., De Roo, A., De Wit, S., Deforche, K., Echahidi, F., Fransen, K., Goffard, J.C., Goubau, P., Goudeseune, E., Yombi, J.C., Lacor, P., Liesnard, C., Moutschen, M., Pierard, D., Rens, R., Schrooten, Y., Vaira, D., Van den Heuvel, A., Van Der Gucht, B., Van Ranst, M., Van Wijngaerden, E., Vandercam, B., Vekemans, M., Verhofstede, C., Clumeck, N., Vandamme, A.M., Van Laethem, K., 2008. Prevalence and epidemiology of HIV type 1 drug resistance among newly diagnosed therapy-naive patients in Belgium from 2003 to 2006. AIDS Res. Hum. Retroviruses 24, 355–362.

Vercauteren, J., Wensing, A.M., van de Vijver, D.A., Albert, J., Balotta, C., Hamouda, O., Kücherer, C., Struck, D., Schmit, J.C., Asjö, B., Bruckova, M., Camacho, R.J., Clotet, B., Coughlan, S., Grossman, Z., Horban, A., Korn, K., Kostrikis, L., Nielsen, C., Paraskevis, D., Poljak, M., Puchhammer-Stockl, E., Riva, C., Ruiz, L., Salminen, M., Schuurman, R., Sonnerborg, A., Stanekova, D., Stanojevic, M., Vandamme,

A.M., Boucher, C.A., 2009. Transmission of drug-resistant HIV-1 is stabilizing in Europe. J. Infect. Dis. 200, 1503–1508.
Wheeler, W.H., Ziebell, R.A., Zabina, H., Pieniazek, D., Prejean, J., Bodnar, U.R., Mahle, K.C., Heneine, W., Johnson, J.A., Hall, H.I., 2010. Prevalence of transmitted drug resistance associated mutations and HIV-1 subtypes in new HIV-1 diagnoses U.S.-2006. AIDS 24, 1203–1212.
Zajdenverg, R., Badal-Faesen, S., Andrade-Villanueva, J., 2009. Lopinavir/ritonavir (LPV/r) tablets administered once- (QD) or twice-daily (BID) with NRTIs in antiretroviral-experienced HIV-1 infected subjects: results of a 48-week randomized trial (study M06-802). In: 5th IAS Conference on HIV Pathogenesis, Treatment and Prevention, Cape Town, South Africa.

High Performance Liquid Chromatography Using UV Detection for the Simultaneous Quantification of the New Non-nucleoside Reverse Transcriptase Inhibitor Etravirine (TMC-125), and 4 Protease Inhibitors in Human Plasma

Atsushi HIRANO,[a,b,c] Masaaki TAKAHASHI,*[,a,b] Eri KINOSHITA,[a] Masaaki SHIBATA,[a] Toshiharu NOMURA,[a] Yoshiyuki YOKOMAKU,[b] Motohiro HAMAGUCHI,[b] and Wataru SUGIURA[b]

[a] *Department of Pharmacy, National Hospital Organization Nagoya Medical Center;* [b] *Clinical Research Center, National Hospital Organization Nagoya Medical Center; 4–1–1 Sannomaru, Naka-ku, Nagoya, Aichi 460–0001, Japan: and* [c] *Department of Medicinal Informatics, Graduate School of Medicine, Kanazawa University; 13–1 Takara-machi, Kanazawa, Ishikawa 920–8640, Japan.*

Received March 4, 2010; accepted May 10, 2010; published online May 20, 2010

Etravirine (TMC-125, ETV) is a second-generation non-nucleoside reverse transcriptase inhibitor (NNRTI) that demonstrates potent activity against NNRTI-resistant strains of human immunodeficiency virus type-1 (HIV-1). Thus, ETV has been used in combination with ritonavir-boosted protease inhibitor (PI) and integrase inhibitor for therapy-experienced HIV-1-infected patients. On the other hand, as ETV is a substrate and inducer of cytochrome P450 3A4 (CYP3A4), ETV may induce metabolism of PI and alter the concentrations of co-administered PIs. In order to ensure optimal drug efficacy and prevention of resistance, it is essential to monitor plasma concentrations of ETV and PIs. Here we describe the application of HPLC with UV detection for the simulataneous assay of ETV and 4 PIs, darunavir (DRV), atazanavir (ATV), ritonavir (RTV) and lopinavir (LPV). In this study, the calibration curve of each drug was linear with the average accuracy ranging from 93.6 to 110.9%. Both intra- and interday coefficients of variation for each drug were less than 11.6%. The mean recovery of all drugs ranged from 88.0 to 97.5%. The limit of quantification was 0.04, 0.04, 0.04, 0.05 and 0.07 μg/ml for ETV, DRV, ATV, RTV and LPV, respectively. These results demonstrate that our HPLC-UV method can be used for routine determination of plasma concentrations of ETV and 4 PIs in clinical settings.

Key words etravirine; HPLC; protease inhibitor; therapeutic drug monitoring

Etravirine (TMC-125, ETV) is a second-generation non-nucleoside reverse transcriptase inhibitor (NNRTI) that demonstrates potent activity against NNRTI-resistant strains of human immunodeficiency virus type-1 (HIV-1). According to the DUET studies (randomized, double-blind, placebo-controlled trials), overall, ETV was well tolerated in treatment-experienced patients infected with HIV-1, with its safety and tolerability profile generally comparable to placebo at week 24.[1,2] Additionally, 48-week data pooled from these studies showed greater virologic and immunologic responses compared with placebo.[3]

In the latest HIV treatment, ETV has been used in combination with ritonavir-boosted protease inhibitor (PI) and integrase inhibitor for therapy-experienced HIV-1-infected patients. On the other hand, as ETV is a substrate and inducer of cytochrome P450 3A4 (CYP3A4), ETV may induce metabolism of PI and alter the concentrations of co-administered PIs.[4] In order to ensure optimal drug efficacy and prevention of resistance, it is essential to monitor plasma concentrations of ETV and PIs.

Fayet *et al.*[5] and Quaranta *et al.*[6] succeeded in determining plasma concentrations of ETV and other drugs through the use of liquid chromatography-tandem mass spectrometry (LC-MS/MS). Rezk *et al.*[7] have also developed a method to measure plasma concentrations of ETV and PIs by LC-MS. LC-MS or LC-MS/MS assay is very sensitive and accurate. However, MS equipment is very expensive and unavailable in conventional hospital laboratories. Therefore, development of alternate methods is necessary.

Recently, D'Avolio *et al.*[8] reported a new HPLC method that employs a photo diode array (HPLC-PDA) for quantification of ETV and other antiretroviral drugs. This method is simple, reliable, and sensitive, using cost-effective instrumentation when compared with others.[5—7] However, this method requires a solid phase extraction. Furthermore, in general hospitals, a UV detector coupled with HPLC is more popular than a PDA detector. The HPLC-UV method is a user-friendly assay that is readily adaptable to standard laboratory equipment for routine therapeutic drug monitoring (TDM).

In this study, we propose the simultaneous quantitative assay of ETV and 4PIs, darunavir (DRV), atazanavir (ATV), ritonavir (RTV) and lopinavir (LPV) in a simple procedure that is derived from a previously established HPLC-UV method.[9] This method can be applied to pharmacokinetic studies of PIs and ETV, the newest NNRTI, and it is useful when evaluating the clinical significance of TDM for these drugs.

MATERIALS AND METHODS

Chemicals ETV and DRV were supplied by Tibotec Pharmaceuticals Ltd. (Eastgate Village, Eastgate, Little Island, Co., Cork, Ireland). LPV and RTV were generously provided by Abbott Laboratories (Abbott Park, IL, U.S.A). ATV was provided by Bristol-Myers Squibb Pharmaceutical Research Institute (New Brunswick, NJ, U.S.A.). The internal standard (IS), 6,7-dimethyl-2,3-di(2-pyridyl)quinoxaline, was purchased from Sigma-Aldrich (St. Louis, MO, U.S.A.). Acetonitrile, methanol, ethyl acetate and *n*-hexane (Kanto

* To whom correspondence should be addressed. e-mail: masaakit@nnh.hosp.go.jp

Chemical, Tokyo, Japan) were HPLC grade. Sodium carbonate was purchased from Katayama Chemical (Osaka, Japan). Water was deionized and osmosed using a Milli-Q® system (Millipore, Bedford, MA, U.S.A.). All other chemicals were of analytical grade and have been described in our previous report.[9]

Standard Solutions Stock solutions of tested drugs and IS were prepared by accurately dissolving weighed amounts of each reference compound in water/ethanol (50 : 50, v/v) to yield concentrations of 191.0 μg/ml for ETV, 85.2 μg/ml for DRV, 502.0 μg/ml for ATV, 425.0 μg/ml for RTV, 95.1 μg/ml for LPV, and 588.0 μg/ml for IS. These stock solutions were stored at −80 °C until the day of analysis. Each stock solution was diluted in drug-free plasma to yield concentrations of 0.08, 0.14, 0.42, 1.04 and 4.17 μg/ml for ETV, 0.07, 0.12, 0.37, 0.93 and 3.72 μg/ml for DRV, 0.09, 0.15, 0.44, 1.10 and 4.38 μg/ml for ATV, 0.07, 0.12, 0.37, 0.93 and 3.71 μg/ml for RTV, 0.08, 0.14, 0.42, 1.04 and 4.15 μg/ml for LPV.

Chromatography The HPLC system consisted of a Waters pump (model 515), a 717 plus autosampler, and a 2487 dual λ absorbance detector coupled to the Empower™ software (Waters, Milford, MA, U.S.A.). The analytical column was a Radial-Pak Nova-Pak C_{18} column (4 μm, 8×100 mm, Waters) protected by Guard-Pak Inserts Nova-Pak C_{18} precolumn. Absorbance was measured at 205 nm, with separations performed at 30 °C. The mobile phase consisted of 39% 50 mM phosphate buffer (pH 6.2), 22% methanol and 39% acetonitrile. The assay run time was 30 min with a flow rate of 1.8 ml/min. Drugs were quantified by measuring the peak areas under the chromatograms.

Sample Preparation A total of 2 ml of ethyl acetate/*n*-hexane (50 : 50, v/v) containing the IS (1.18 μg/ml) and 1 ml of 0.5 M sodium carbonate were added to a 500 μl plasma sample. The mixture was vortexed and then centrifuged at 3500×*g* for 5 min. The organic layer was separated and evaporated to dryness. The dried material was then dissolved in 100 μl of a mobile phase solution and centrifuged at 13000×*g* for 5 min. Lastly, 25 μl of the upper solution was injected into the HPLC column.

The institutional review board of the National Hospital Organization Nagoya Medical Center approved this study. Plasma samples were prepared from patients after obtaining written informed consent.

Validation Intra- and interday precision values using this method were estimated by assaying control plasma containing five different concentrations of each drug five times on the same day and on three separate days to obtain the coefficient of variation (CV). Accuracy was determined as the percentage of the nominal concentration. Drug recovery from plasma was evaluated by analyzing triplicate samples with or without extraction. Plasma samples spiked with known amounts of both drugs and IS were extracted as usual. Blank plasma samples that contained only the IS were extracted and subsequently spiked with the same amount of analytes to give the 100% reference. The recovery was assessed by comparing the peak area ratio (analytes/IS) of extracts. The limit of quantification was defined as the lowest concentration for which both the CV% and the percent of deviation from the nominal concentration were less than 20%.

RESULTS

Plasma Sample Chromatograms Figure 1A is a chromatogram of a spiked plasma sample containing 3.77 μg/ml of DRV, 1.18 μg/ml of IS, 4.44 μg/ml of ATV, 3.76 μg/ml of RTV, 1.69 μg/ml of ETV and 4.21 μg/ml of LPV. Under the described chromatographic conditions, retention times were 3.4, 4.4, 8.3, 10.5, 11.7, 13.0 min for DRV, IS, ATV, RTV, ETV and LPV, respectively. At a detection wavelength of 205 nm, assays performed on drug-free human plasma demonstrated that there were no interfering peaks during the intervals of interest for the retention times (Fig. 1B).

Figure 2A is a chromatogram of a plasma sample from an HIV-1-infected patient treated with raltegravir, ETV, ATV, RTV and lamivudine. The patient was a Japanese male aged 37 years with a body weight of 72.6 kg. His $CD4^+$ T cell count was 302/μl with a viral load of 7200 copies/ml. ETV and other antiretroviral agents were administered for 7 d. The plasma concentration at trough was 0.30, 0.48 and 0.24 μg/ml for ETV, ATV and RTV, respectively.

Figure 2B shows a chromatogram of a plasma sample from an HIV-1-infected patient treated with raltegravir, ETV, DRV, RTV and lamivudine. The patient was a Brazilian male aged 49 years with a body weight of 83.0 kg. His $CD4^+$ T cell count was 157/μl with a viral load of 44 copies/ml. ETV

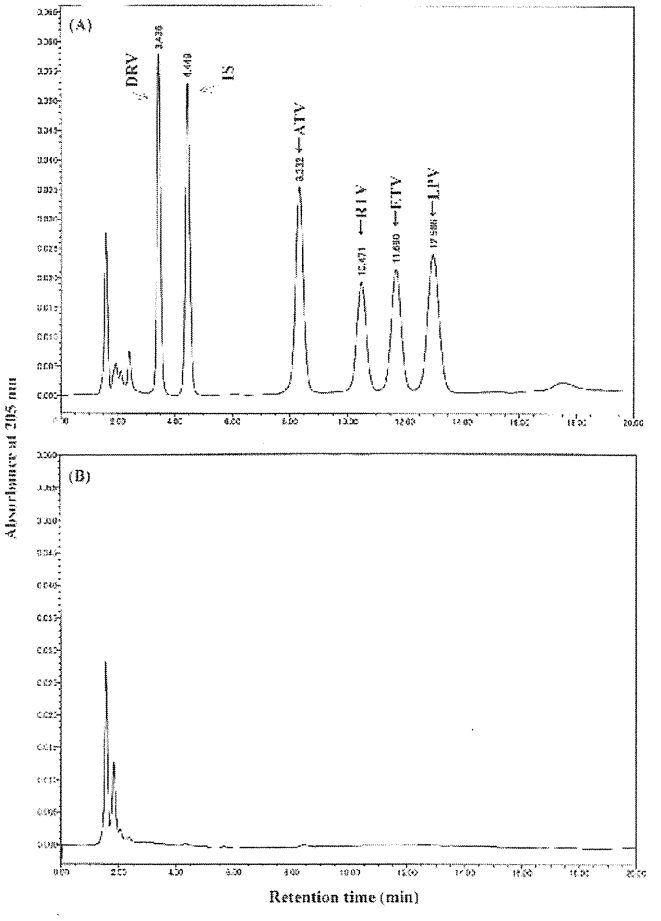

Fig. 1. Chromatograms Obtained after Extraction of (A) Spiked Plasma Sample Containing 3.77 μg/ml of DRV, 1.18 μg/ml of IS, 4.44 μg/ml of ATV, 3.76 μg/ml of RTV, 1.69 μg/ml of ETV and 4.21 μg/ml of LPV, and (B) Drug-Free Human Plasma Sample from a Healthy Volunteer

DRV, darunavir; IS, internal standard; ATV, atazanavir; RTV, ritonavir; ETV, etravirine; LPV, lopinavir.

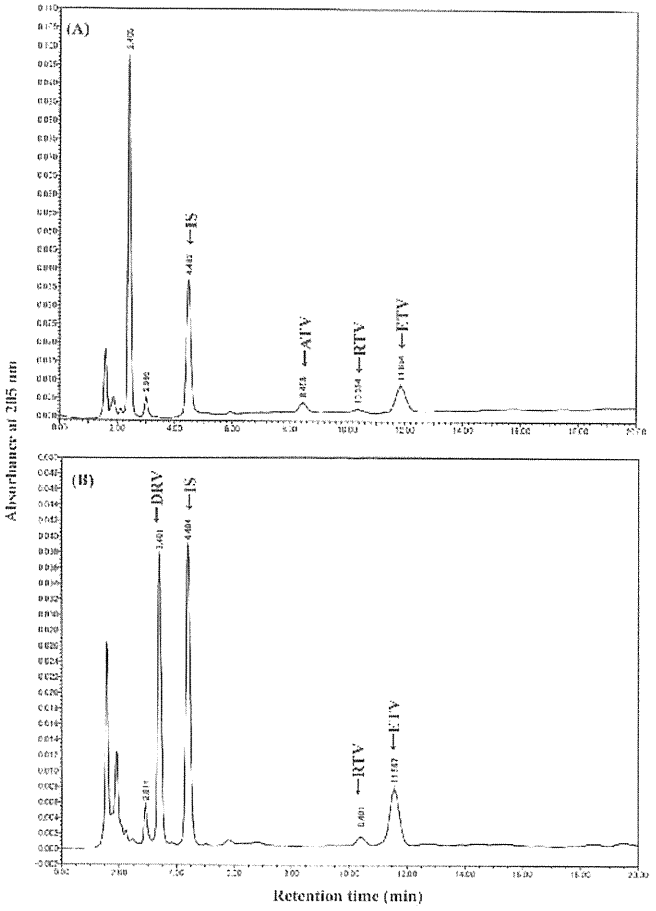

Fig. 2. Chromatograms Obtained after Extraction of a Plasma Sample from an HIV-1-Infected Patient (A) Treated with Raltegravir, ETV, ATV, RTV and Lamivudine, and (B) Treated with Raltegravir, DRV, ETV, RTV and Lamivudine

DRV, darunavir; IS, internal standard; ATV, atazanavir; RTV, ritonavir; ETV, etravirine.

and other antiretroviral agents were administered for 3 weeks. The plasma concentration at trough was 0.33, 3.30, and 0.29 μg/ml for ETV, DRV and RTV, respectively.

In chromatograms of Figs. 2A and B, the peaks of raltegravir and lamivudine were not detected.

Precision, Accuracy, Recovery, Linearity and Limit of Quantification The precision and accuracy for all tested drugs are shown in Table 1. The analyses show satisfactory precision with intra- and interassay coefficients of variation less than 11.6%. Accuracies ranged from 93.6 to 110.9%. The mean recovery of all drugs ranged from 88.0 to 97.5%. The regression coefficients of determination (R^2) values of the calibration curves for each drug were 0.99 or greater. The limit of quantification was 0.04, 0.04, 0.04, 0.05 and 0.07 μg/ml for ETV, DRV, ATV, RTV and LPV, respectively.

Table 1. Intra- and Interday Precision and Accuracy for ETV, ATV, RTV, LPV and DRV

	Expected (μg/ml)	Intraday ($n=5$) Measured (μg/ml)	CV (%)	Interday ($n=15$) Measured (μg/ml)	CV (%)	Accuracy (%)
ETV	0.08	0.09±0.00	3.0	0.09±0.00	4.9	110.9±2.8
	0.14	0.14±0.01	3.9	0.14±0.01	3.9	99.4±3.9
	0.42	0.42±0.01	1.2	0.42±0.01	3.0	99.8±3.0
	1.04	1.03±0.01	0.5	1.03±0.01	1.4	98.9±1.4
	4.17	4.17±0.03	0.8	4.14±0.05	1.3	99.2±1.2
ATV	0.09	0.09±0.00	2.2	0.09±0.01	6.5	103.1±6.7
	0.15	0.16±0.00	2.6	0.16±0.01	3.3	103.6±3.4
	0.44	0.45±0.01	1.4	0.44±0.01	2.4	100.8±2.5
	1.10	1.10±0.00	0.4	1.12±0.02	2.1	101.4±2.1
	4.38	4.37±0.01	0.3	4.38±0.04	0.9	99.9±0.9
RTV	0.07	0.07±0.01	8.1	0.07±0.01	8.0	93.6±7.5
	0.12	0.12±0.00	3.3	0.12±0.01	4.4	100.3±4.4
	0.37	0.37±0.01	2.3	0.37±0.01	3.9	99.6±3.9
	0.93	0.93±0.01	1.4	0.94±0.02	2.2	101.1±2.2
	3.71	3.72±0.07	1.9	3.69±0.06	1.7	99.6±1.6
LPV	0.08	0.08±0.01	11.6	0.09±0.01	9.3	107.3±10.0
	0.14	0.14±0.00	2.7	0.14±0.01	3.7	99.2±3.7
	0.42	0.42±0.01	2.7	0.42±0.01	3.4	101.1±3.9
	1.04	1.04±0.01	0.8	1.05±0.02	2.1	100.5±2.1
	4.15	4.14±0.02	0.4	4.16±0.07	1.6	100.1±1.6
DRV	0.07	0.07±0.01	7.6	0.08±0.01	9.9	108.4±10.7
	0.12	0.12±0.01	4.7	0.12±0.00	3.9	99.7±3.9
	0.37	0.37±0.01	1.9	0.37±0.01	2.8	100.8±2.8
	0.93	0.93±0.01	0.9	0.93±0.02	1.9	100.5±1.9
	3.72	3.70±0.04	1.0	3.72±0.03	0.9	100.1±0.9

ETV, etravirine; ATV, atazanavir; RTV, ritonavir; LPV, lopinavir; DRV, darunavir; CV, coefficient of variation.

DISCUSSION

ETV has activity *in vitro* against viral strains with mutations that confer resistance to efavirenz and nevirapine.[11] The EC_{50} of ETV was <100 nM (43.5 ng/ml) against clinically derived recombinant viruses resistant to at least one of the currently marketed NNRTIs. However, clinical investigations have yet to determine the therapeutic range of ETV concentrations that are associated with the desired therapeutic response. In addition, there is the potential problem for complex drug interactions due to the fact that ETV is a substrate and inducer of CYP3A4, as well as a substrate and inhibitor of 2C9 and 2C19.[4] In clinical treatment, ETV is coadministered with other antiretroviral agents including RTV-boosted PI. Therefore, too-low or too-high plasma concentrations of these drugs may decrease treatment efficacy or increase the risk of adverse effects. To solve these problems, a simple drug monitoring system for these agents is needed. Here we describe the application of HPLC with UV detection for simultaneously assaying ETV and 4 PIs. HPLC-UV equipment is frequently used in conventional hospital laboratories.

In this study, the calibration curve of each drug was linear with the average accuracy ranging from 93.6 to 110.9%. Both intra- and interday coefficients of variation for each drug were less than 11.6%. These results demonstrate that our HPLC-UV method has advantages in both reproduciblity and accuracy in measuring plasma concentration of ETV and 4 PIs in a single run.

In our clinical cases, the ETV plasma concentrations, measured at trough, were 0.30 or 0.33 μg/ml for the HIV-1-infected patients. These values were similar to the previously reported findings in DUET studies.[1,2] In each case, the trough concentration of DRV or ATV was more than the suggested minimum target trough value in the guideline.[4] The viral load has been decreasing in these patients and treatment success is expected in the future. We, thus, proposed maintaining the current daily dose of these drugs. Conversely, the peaks of co-administered raltegravir and lamivudine were not

detected because these drugs were not extracted from plasma by our liquid–liquid extraction technique. As these drugs are not metabolized by cytochrome P450, there are no drug interactions with ETV.

In conclusion, we have successfully constructed a protocol for the simultaneous quantification of ETV and 4 PIs by HPLC-UV. We believe our method enables accurate monitoring of ETV and co-administered PIs and may guide optimized administration of these drugs and prevent potential drug interactions and toxicity in treatment.

Acknowledgments This study was supported in part by a Grant-in-Aid for Clinical Research from the National Hospital Organization to MT. Janssen Pharmaceutical K.K. also provided funding for this study.

REFERENCES AND NOTES

1) Madruga J. V., Cahn P., Grinsztejn B., Haubrich R., Lalezari J., Mills A., Pialoux G., Wilkin T., Peeters M., Vingerhoets J., de Smedt G., Leopold L., Trefiglio R., Woodfall B., *Lancet*, **370**, 29—38 (2007).
2) Lazzarin A., Campbell T., Clotet B., Johnson M., Katlama C., Moll A., Towner W., Trottier B., Peeters M., Vingerhoets J., de Smedt G., Baeten B., Beets G., Sinha R., Woodfall B., *Lancet*, **370**, 39—48 (2007).
3) Katlama C., Haubrich R., Lalezari J., Lazzarin A., Madruga J. V., Molina J. M., Schechter M., Peeters M., Picchio G., Vingerhoets J., Woodfall B., De Smedt G., *AIDS*, **23**, 2289—2300 (2009).
4) The Panel on Clinical Practices for Treatment of HIV Infection Convened by the Department of Health and Human Services (DHHS), Published at http://AIDSinfo.nih.gov, 1 December 2009.
5) Fayet A., Beguin A., Zanolari B., Cruchon S., Guignard N., Telenti A., Cavassini M., Gunthard H. F., Buclin T., Biollaz J., Rochat B., Decosterd L. A., *J. Chromatogr. B, Analyt. Technol. Biomed. Life Sci.*, **877**, 1057—1069 (2009).
6) Quaranta S., Woloch C., Paccou A., Giocanti M., Solas C., Lacarelle B., *Ther. Drug Monit.*, **31**, 695—702 (2009).
7) Rezk N. L., White N. R., Jennings S. H., Kashuba A. D., *Talanta*, **79**, 1372—1378 (2009).
8) D'Avolio A., Baietto L., Siccardi M., Sciandra M., Simiele M., Oddone V., Bonora S., Di Perri G., *Ther. Drug Monit.*, **30**, 662—669 (2008).
9) Takahashi M., Yoshida M., Oki T., Okumura N., Suzuki T., Kaneda T., *Biol. Pharm. Bull.*, **28**, 1286—1290 (2005).
10) Product Information, INTELENCE (etravirine tablet), Tibotec Therapeutics, Bridgewater, NJ, U.S.A.: http://www.intelence-info.com/intelence/
11) Andries K., Azijn H., Thielemans T., Ludovici D., Kukla M., Heeres J., Janssen P., De Corte B., Vingerhoets J., Pauwels R., de Bethune M. P., *Antimicrob. Agents Chemother.*, **48**, 4680—4686 (2004).

JOURNAL OF VIROLOGY, Oct. 2010, p. 9995–10003
0022-538X/10/$12.00 doi:10.1128/JVI.00505-10

Vol. 84, No. 19

The Effect of Clade-Specific Sequence Polymorphisms on HIV-1 Protease Activity and Inhibitor Resistance Pathways[▽]

Rajintha M. Bandaranayake,[1] Madhavi Kolli,[1] Nancy M. King,[1] Ellen A. Nalivaika,[1] Annie Heroux,[2] Junko Kakizawa,[3] Wataru Sugiura,[3,4] and Celia A. Schiffer[1]*

Department of Biochemistry and Molecular Pharmacology, University of Massachusetts Medical School, 364 Plantation Street, Worcester, Massachusetts 01605[1]; Biology Department, Brookhaven National Laboratory, Upton, New York 11973-5000[2]; Laboratory of Therapeutic Research and Clinical Science, AIDS Research Center, National Institute of Infectious Diseases, 4-7-1 Gakuenn, Musashimurayama, Tokyo 208-0011, Japan[3]; and Department of Infection and Immunology, Clinical Research Center, Nagoya Medical Center, Nagoya, Japan[4]

Received 6 March 2010/Accepted 14 July 2010

The majority of HIV-1 infections around the world result from non-B clade HIV-1 strains. The CRF01_AE (AE) strain is seen principally in Southeast Asia. AE protease differs by ~10% in amino acid sequence from clade B protease and carries several naturally occurring polymorphisms that are associated with drug resistance in clade B. AE protease has been observed to develop resistance through a nonactive-site N88S mutation in response to nelfinavir (NFV) therapy, whereas clade B protease develops both the active-site mutation D30N and the nonactive-site mutation N88D. Structural and biochemical studies were carried out with wild-type and NFV-resistant clade B and AE protease variants. The relationship between clade-specific sequence variations and pathways to inhibitor resistance was also assessed. AE protease has a lower catalytic turnover rate than clade B protease, and it also has weaker affinity for both NFV and darunavir (DRV). This weaker affinity may lead to the nonactive-site N88S variant in AE, which exhibits significantly decreased affinity for both NFV and DRV. The D30N/N88D mutations in clade B resulted in a significant loss of affinity for NFV and, to a lesser extent, for DRV. A comparison of crystal structures of AE protease shows significant structural rearrangement in the flap hinge region compared with those of clade B protease and suggests insights into the alternative pathways to NFV resistance. In combination, our studies show that sequence polymorphisms within clades can alter protease activity and inhibitor binding and are capable of altering the pathway to inhibitor resistance.

Human immunodeficiency virus type 1 (HIV-1) is classified into three groups (M, N, and O), of which group M is further classified into nine major clades (A, B, C, D, F, G, H, J, and K) and 43 circulating recombinant forms (CRFs) based on viral genomic diversity (32, 37). The majority of HIV-1 infections across the globe result from non-B clade HIV-1 variants; clade B accounts for only ~12% of infections (15). However, the development of currently available anti-HIV therapies has been based on the virology of clade B variants. In recent years, several studies have shown that there are clear differences between clades when it comes to viral transmission and the progression to AIDS, an observation which raises questions about the effectiveness of the currently available anti-HIV therapies against the other clades and CRFs (16–18, 39).

HIV-1 protease has been an important drug target in the global effort to curb the progression from HIV infection to AIDS. However, the accumulation of drug-resistant mutations in the protease gene has been a major drawback in using HIV-1 protease inhibitors. The effects of mutations associated with drug resistance in HIV-1 clade B protease have been studied extensively over the years. For the most part, resistance mutation patterns are very similar in HIV-1 clade B and non-B clade proteases (19). However, several alternative resistance pathways have been observed for non-B clade proteases compared with those of clade B protease (1, 12, 13, 26). Limited data are available on how sequence polymorphisms, some of which are associated with drug resistance in clade B protease, might influence the pathway to drug resistance in non-B clade proteases. Furthermore, very little is understood about how sequence polymorphisms in non-B clade proteases affect protease function and inhibitor binding.

HIV-1 CRF01_AE (AE) was the first CRF to be observed in patient populations and is seen principally in Southeast Asia (2, 10, 25). AE protease differs by ~10% in amino acid sequence from that of clade B protease (Fig. 1A). Interestingly, AE protease develops a different resistance pathway from that of clade B protease to confer resistance to the protease inhibitor nelfinavir (NFV) (1). In patients infected with AE, the protease acquires predominantly the N88S mutation in response to NFV therapy, whereas in patients with clade B infection, the protease acquires the D30N/N88D mutations. The fitness of AE viral strains is thought to be similar to that of HIV-1 group M viral strains (11, 41). However, the effect of AE-specific sequence variations as well as drug resistance substitutions on viral fitness has not been studied extensively.

In the present study, biochemical and biophysical methods were used to determine the effect of sequence polymorphisms in AE protease on enzyme activity and inhibitor binding. Through determination of crystal structures and analysis of changes in hydrogen bonding patterns, a structural rationalization is described for the two different pathways observed for clade B and AE proteases to attain resistance to NFV.

* Corresponding author. Mailing address: Department of Biochemistry and Molecular Pharmacology, University of Massachusetts Medical School, 364 Plantation Street, Worcester, MA 01605. Phone: (508) 856-8008. Fax: (508) 856-6464. E-mail: Celia.Schiffer@umassmed.edu.
▽ Published ahead of print on 21 July 2010.

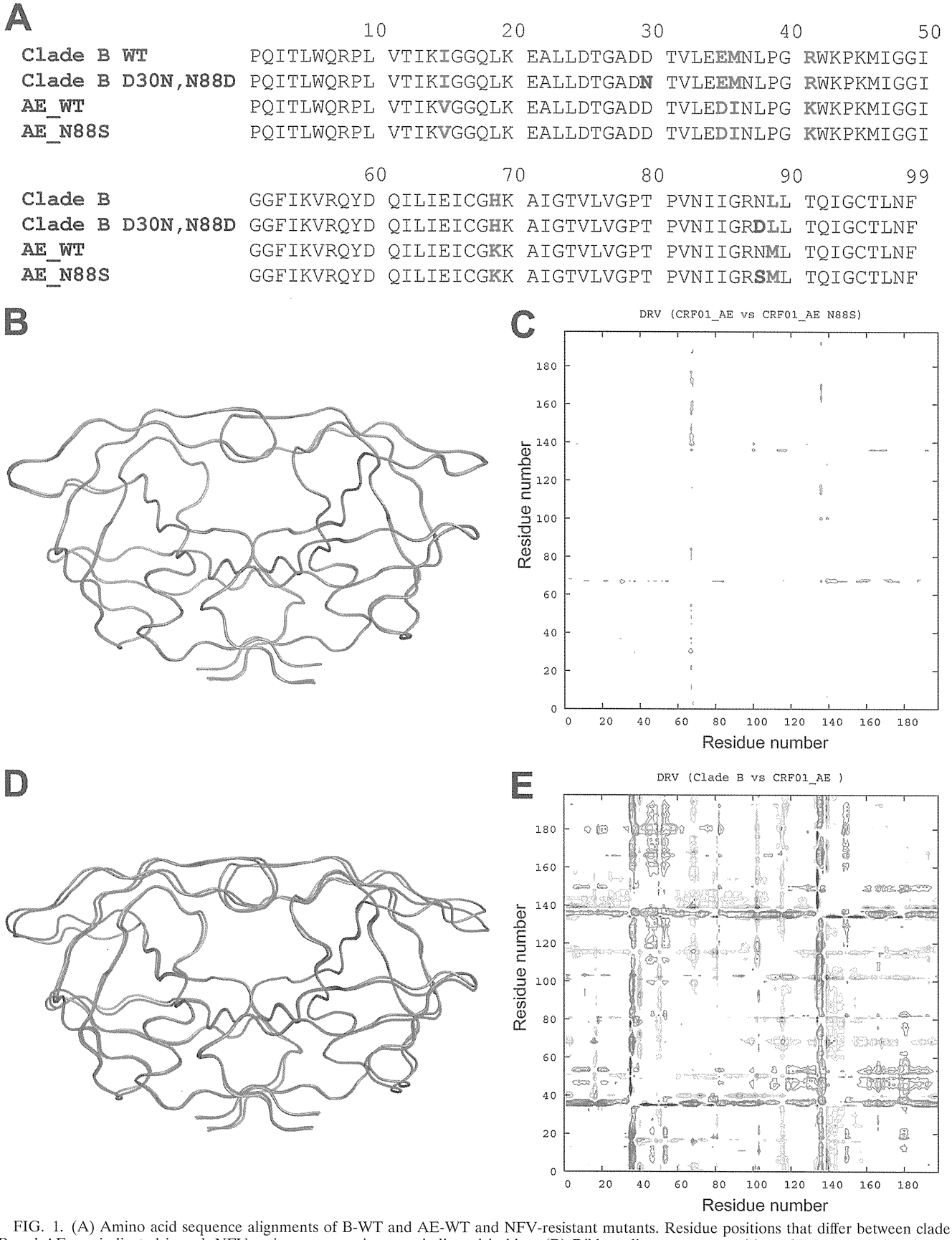

FIG. 1. (A) Amino acid sequence alignments of B-WT and AE-WT and NFV-resistant mutants. Residue positions that differ between clade B and AE are indicated in red. NFV resistance mutations are indicated in blue. (B) Ribbon diagram superposition of $DRV_{AE\text{-}WT}$ (blue) and $DRV_{AE\text{-}N88S}$ (gray). (C) Double-difference plot comparing $DRV_{AE\text{-}WT}$ and $DRV_{AE\text{-}N88S}$. (D) Ribbon diagram superposition of clade $DRV_{AE\text{-}WT}$ (magenta) and clade $DRV_{B\text{-}WT}$ (gray). (E) Double-difference plot comparing $DRV_{AE\text{-}WT}$ and $DRV_{B\text{-}WT}$. The color contours in the double-difference plots indicate distance differences of <1.0 Å (black), 1.0 to 0.5 Å (green), 0.5 to 1.0 Å (blue), and >1.0 Å (red).

MATERIALS AND METHODS

Protease gene construction. The clade B wild-type (B-WT) protease gene was generated as previously described (34). The AE wild-type (AE-WT) protease gene was synthesized in fragments (Integrated DNA Technologies, Coralville, IA), with codons optimized for expression in *Escherichia coli*. The fragments were ligated to form the complete gene, which was then inserted into the pET11a expression vector (Novagen/EMD Chemicals, Gibbstown, NJ). The protease sequence was confirmed by DNA sequencing. The NFV resistance mutations, N88S in AE (AE-N88S) and D30N/N88D in clade B (B-D30N/N88D), were generated by site-directed mutagenesis using a Stratagene QuikChange site-directed mutagenesis kit (Agilent Technologies, La Jolla, CA). Mutagenesis was confirmed by sequencing. The Q7K substitution was introduced to all protease variants to prevent autoproteolysis (38).

Protein expression and purification. The clade B and AE variants were subcloned into the heat-inducible pXC35 expression vector (American Type Culture Collection [ATCC], Manassas, VA) and transformed into *E. coli* TAP-106 cells. Protein overexpression, purification, and refolding were carried out as previously described (20). Protein used for crystallographic studies was further purified with a Pharmacia Superdex 75 fast-performance liquid chromatography column (GE Healthcare, Chalfont St. Giles, United Kingdom) equilibrated with refolding buffer (50 mM sodium acetate [pH 5.5], 10% glycerol, 5% ethylene glycol, and 5 mM dithiothreitol).

Crystallization and structure determination. Protease solutions between 1.0 and 2.0 mg ml^{-1} were equilibrated with a 5-fold molar excess of NFV, darunavir (DRV), and amprenavir (APV) for 1 h on ice. Crystals were grown over a reservoir solution consisting of 126 mM phosphate buffer (pH 6.2), 63 mM sodium citrate, and 18% to 23% ammonium sulfate by the hanging-drop vapor diffusion method. X-ray diffraction data for AE-WT were collected at a BioCARS beamline 14-BM-C at the Advanced Photon Source (Argonne National Laboratory, Argonne, IL) at a wavelength tuned to 0.9 Å with a Quantum 315 CCD X-ray detector (Area Detector Systems Corporation, Poway, CA). Diffraction data for AE-N88S were collected by using beamline X29A at the National Synchrotron Light Source (Brookhaven National Laboratory, Upton, NY) at a wavelength tuned to 1.08 Å with a Quantum 315 charge-coupled-device (CCD) X-ray detector (Area Detector Systems Corporation). Data for the B-D30N/N88D variant was collected in-house with an R-Axis IV imaging plate system (Rigaku Corporation, Tokyo, Japan) mounted on a rotating-anode X-ray source (Rigaku Corporation). All data were collected under cryocooled conditions.

The data were indexed, integrated, and scaled using HKL/HKL-2000 software (HKL Research, Charlottesville, VA) (29). Structure determination and refinement were carried out using the CCP4 program suite (4) as previously described (35). The tensor (T), libration (L), and screw (S) parameter files used in TLS refinement were generated using the TLS motion determination server (30). Model building and real-space refinement were carried out with Coot molecular graphics software (8). Structure comparisons were made by superposing the structures using the Cα atoms of the terminal regions (residues 1 to 9 and 86 to 99) from the two monomers. In the case of the AE complexes, which have multiple orientations for the inhibitor, only the orientation common with the clade B structures was used for analysis. Structures were visualized using PyMol molecular graphics software (6).

Double-difference plots were generated for AE and clade B protease structures to graphically visualize structural differences between the clades, as previously described (35). Briefly, distances between all Cα atoms within the dimer were calculated for each complex. A distance difference matrix was then computed for each atom for a given pair of complexes. The distance difference matrix was then plotted as a contour plot using the gnuplot plotting software (44).

Nomenclature. The following nomenclature format will be used to refer to each crystal structure: $\text{inhibitor}_{\text{protease variant}}$. Thus, DRV in complex with AE-WT, clade B-WT, AE-N88S, and AE-D30N/N88D protein are designated $DRV_{AE\text{-}WT}$, $DRV_{B\text{-}WT}$, $DRV_{AE\text{-}N88S}$, and $DRV_{B\text{-}D30N/N88D}$, respectively. Prime notation is used to distinguish the two monomers in the protease dimer. For example, residue 30 from the first monomer would be referred to as Asp30, and the same residue from the second monomer would be referred to as Asp30′.

ITC. Binding affinities and thermodynamic parameters of inhibitor binding to clade B and AE variants were determined by isothermal titration calorimetry (ITC) with a VP isothermal titration calorimeter (MicroCal, LLC, Northampton, MA). The buffer used for all protease and inhibitor solutions consisted of 10 mM sodium acetate (pH 5.0), 2% dimethyl sulfoxide, and 2 mM tris[2-carboxyethyl] phosphine. Binding affinities for all protease variants were obtained by competitive displacement titration using acetyl-pepstatin as the weaker binder. A solution of 30 to 45 μM protease was titrated with 10-μl injections of 200 μM acetyl-pepstatin to saturation. The pepstatin was then displaced by titrating 36 8-μl injections of 200 μM APV or NFV or 41 7-μl injections of 40 μM DRV. Heats of dilution were subtracted from the corresponding heats of reaction to obtain the heat resulting solely from the binding of the ligand to the enzyme. Data were processed and analyzed with the ITC data analysis module (Microcal) for Origin 7 data analysis and graphing software (OriginLab, Northampton, MA). Final results represent the average of at least two measurements.

Measurement of protease activity. Protease activity was assayed by following each variant's ability to hydrolyze the fluorogenic substrate HiLyte Fluor 488-Lys-Ala-Arg-Val-Leu-Ala-Glu-Ala-Met-Ser-Lys (QXL-520) (AnaSpec, Inc., Fremont, CA) that corresponds to the HIV-1 CA-p2 substrate. The CA-p2 cleavage site was used since it is conserved between HIV-1 clades (7). The assay was carried out in a 96-well plate, and the enzymatic reaction was initiated by adding 20 μl of a solution of 100 to 250 nM protease to 80 μl of substrate solution. The buffer used in all reactions consisted of 10 mM sodium acetate (pH 5.0), 2% dimethyl sulfoxide, and 2 mM tris[2-carboxyethyl]phosphine. Final concentrations in each experiment were 0 to 40 μM substrate and 20 to 50 nM protease. Accurate concentrations of properly folded active protease were determined by carrying out ITC experiments for each variant with acetyl-pepstatin as described in the previous section. Fluorogenic response to protease cleavage was monitored at 23°C using a Victor^3 microplate reader (PerkinElmer, Waltham, MA) by exciting the donor molecule at 485 nM and recording emitted light at 535 nM. Data points were acquired every 30 s. The data points in relative fluorescence units (RFU) were converted into concentrations using standard calibration curves generated for HiLyte Fluor 488 at each substrate concentration. In addition to the conversion of RFUs to concentrations, the generation of calibration curves at each substrate concentration allowed us to correct for the inner filter effect (5). Rates of each enzymatic reaction were determined from the linear portion of the data and were fitted against substrate concentrations to determine K_m and catalytic turnover rate (k_{cat}) values using VisualEnyzmics enzyme-kinetics software (SoftZymics, Princeton, NJ). Final results for each variant represent the average from at least two experiments.

In order to determine the biochemical fitness of a particular variant in the presence of a given inhibitor, vitality values were calculated using the following equation, based on the vitality function described previously, where K_d is the dissociation constant and k_{cat}/K_m is the catalytic efficiency (14, 43).

$$\text{Vitality} = \frac{[K_d \times (k_{cat}/K_m)]_{\text{mutant}}}{[K_d \times (k_{cat}/K_m)]_{\text{clade B-WT}}}$$

The calculated vitality value for B-WT for a particular inhibitor would be 1.0, and vitality values greater than 1.0 would indicate that a given variant had a selective advantage over the same inhibitor, while values lower than 1.0 would indicate that the variant did not have a selective advantage.

RESULTS

Crystal structures. The AE-WT and NFV-resistant clade B and AE variants were cocrystallized with NFV, DRV, and APV to reveal the structural basis for the altered NFV resistance pathways. In addition, the effects of background polymorphisms in AE-WT on inhibitor binding compared with that of clade B-WT were discerned. Crystals of AE protease in complex with NFV and APV did not diffract to a high resolution; therefore, structural comparisons were carried out for AE and clade B protease in complex with DRV. The structure of $DRV_{B\text{-}WT}$ was solved previously in the laboratory and was used for structural comparisons (Protein Data Bank [PDB] code 1T3R). Both $DRV_{AE\text{-}WT}$ and $DRV_{AE\text{-}N88S}$ crystallized with DRV bound in two orientations in the active site. Crystallographic data and refinement statistics for $DRV_{AE\text{-}WT}$, $DRV_{B\text{-}WT}$, $DRV_{AE\text{-}N88S}$, and $DRV_{B\text{-}D30N/N88D}$ are given in Table 1.

Structural comparisons were carried out for AE and clade B DRV complexes by pairwise structural superposition and double-difference plots (Fig. 1B to E). The $DRV_{AE\text{-}WT}$ and $DRV_{AE\text{-}N88S}$ complexes were structurally similar (Fig. 1B and C). Although the $DRV_{AE\text{-}WT}$ and $DRV_{B\text{-}WT}$ could be superimposed on each other very well (root mean square deviation

TABLE 1. Crystallographic statistics

Parameter[a]	Result for indicated variant			
	$DRV_{B\text{-}WT}$[b]	$DRV_{B\text{-}D30N/N88D}$	$DRV_{AE\text{-}WT}$	$DRV_{AE\text{-}N88S}$
Inhibitor	DRV	DRV	DRV	DRV
Resolution (Å)	1.2	2.15	1.96	1.76
Space group	$P\ 2_1\ 2_1\ 2_1$	$P\ 2_1\ 2_1\ 2_1$	$P\ 6_1$	$P\ 6_1$
Z	4	4	6	6
Cell dimensions (Å)				
a	54.9	50.9	62.2	61.9
b	57.8	57.7		
c	62.0	61.6	82.7	82.1
Total no. of reflections	302,022	108,838	89,284	79,445
No. of unique reflections	55,056	10,326	12,493	17,277
R_{symm} (%)	3.8	6.7	5.5	4.6
Completeness (%)	95.5	99.6	93.9	97.4
I/σ^I	25.0	9.6	11.2	19.6
R_{work} (%)	14.1	18.1	20.0	19.6
R_{free} (%)	17.9	23.6	25.9	23.9
RMSD				
Bond length (Å)	0.004	0.009	0.009	0.007
Bond angle	1.5	1.9	1.5	1.7
PDB code	1T3R	3LZV	3LZS	3LZU

[a] Z, number of molecules in the unit cell; RMSD, root mean square deviation; $R_{symm} = \Sigma_{hkl}|I_{hkl} - \langle I_{hkl}\rangle|/\Sigma_{hkl}I_{hkl}$; I/σ^I, signal-to-noise ratio; $R_{work} = \Sigma||F_{obs} - F_{cal}||/\Sigma F_{obs}$; $R_{free} = \Sigma_{test}(|F_{obs}| - F_{cal}|)^2/\Sigma_{test}|F_{obs}|^2$.
[b] See King et al.(21) and Surleraux et al. (40).

[RMSD] of 0.21 Å), there were clear and significant differences between the variants in the main chain at the flap hinge region (residues 33 to 39) and the protease core region (residues 16 to 22) (Fig. 1D and Fig. 2A to D). These differences were further evident by the presence of significant peaks in the double-difference plot (Fig. 1E). The Ile36 side chain in $DRV_{AE\text{-}WT}$ packs well against the core region through favorable van der Waals interactions and is shorter than the Met36 in $DRV_{B\text{-}WT}$ (Fig. 2C). In addition, the shorter Asp35 in $DRV_{AE\text{-}WT}$ further enhances the packing by being flipped inward against the core, while in $DRV_{B\text{-}WT}$, the longer Glu35 is flipped outward into the solvent and forms a salt bridge with Arg57 (Fig. 2D). The packing of the flap hinge and core regions in $DRV_{AE\text{-}WT}$ is further stabilized by a hydrogen bond between the carbonyl oxygen of Asp35 and Lys20 NZ atom and is not present in $DRV_{B\text{-}WT}$.

The Asp30′ side chain of $DRV_{B\text{-}WT}$ does not directly form a hydrogen bond with DRV but indirectly interacts with the N1 atom of DRV through a water molecule-mediated hydrogen bond network (Fig. 3A). In contrast, the Asp30′ side chain of $DRV_{AE\text{-}WT}$ forms a direct hydrogen bond with the N1 atom of DRV (Fig. 3B). Residue 30 of both NFV-resistant variants also interacts with the N1 atom of DRV through water molecule-mediated hydrogen bonding (Fig. 3C and D). However, in addition to this interaction, Asn30 of $DRV_{B\text{-}D30N/N88D}$ and Asp30 of $DRV_{AE\text{-}N88S}$ are oriented away from the active site, enabling them to form hydrogen bonds with Asp88 and Ser88, respectively. In both cases, the NFV resistance mutations stabilize residue 30 away from the active site via hydrogen bonding.

Binding thermodynamics. To determine the effects of background sequence polymorphisms and NFV resistance mutations on inhibitor binding, the binding thermodynamic parameters of NFV, DRV, and APV binding to WT and resistant AE and clade B variants were determined by isothermal titration calorimetry (Table 2). The AE-WT protease had a 6.9-fold-weaker affinity for NFV and a 2.7-fold-weaker affinity for DRV

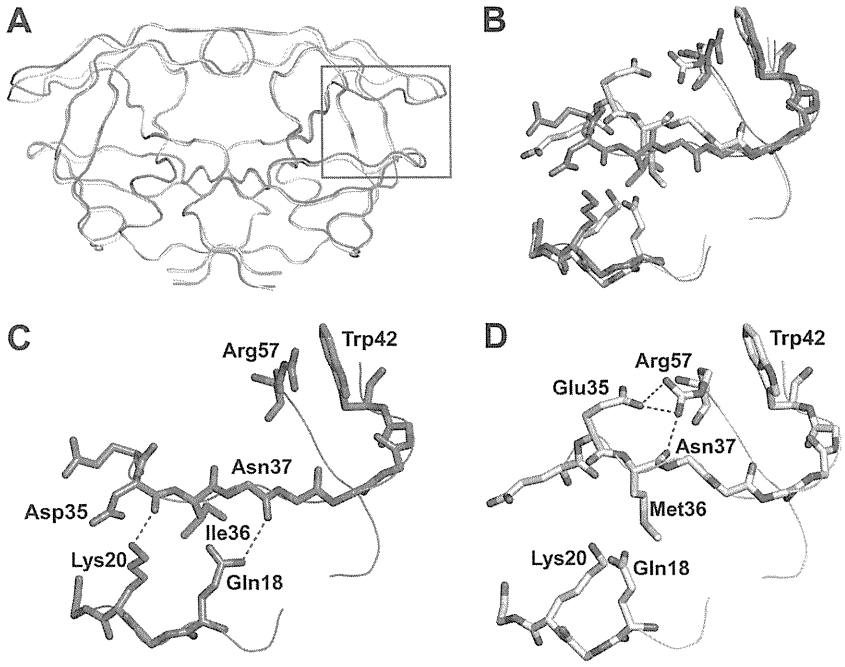

FIG. 2. (A) Ribbon diagram superposition of $DRV_{AE\text{-}WT}$ (blue) and $DRV_{B\text{-}WT}$ (gray). The red box indicates the region of the protease molecule highlighted in panels B to D. (B) Structural rearrangement of the flap hinge and core regions between $DRV_{AE\text{-}WT}$ (blue) and $DRV_{B\text{-}WT}$ (gray). (C) Flap hinge and core regions of $DRV_{AE\text{-}WT}$. (D) Flap hinge and core regions of $DRV_{B\text{-}WT}$ protease. Hydrogen bond interactions are indicated by red dashed lines.

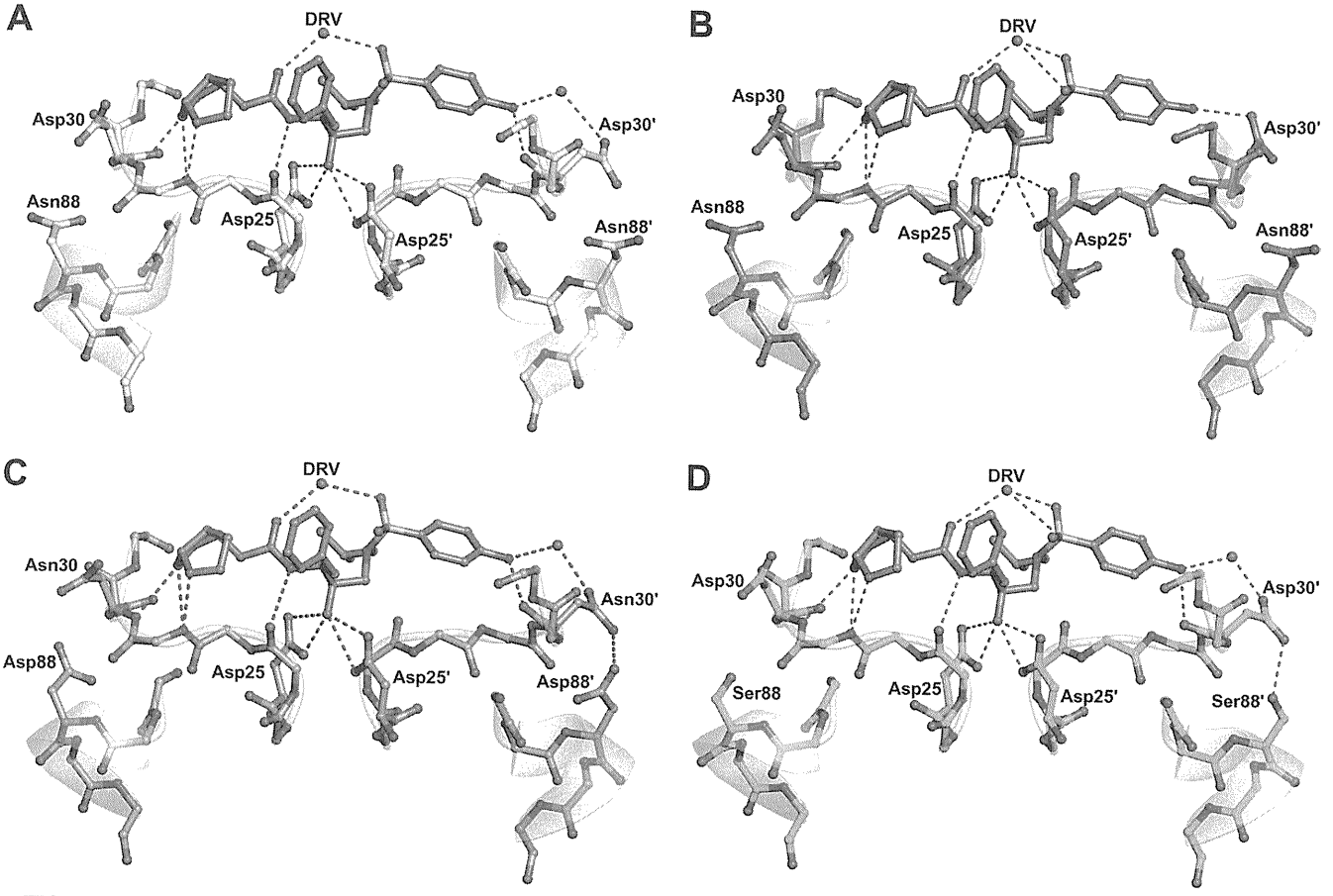

FIG. 3. Protease inhibitor hydrogen bonding interactions. DRV is shown in orange, and hydrogen bond interactions are indicated by red dashed lines. Since the charged states of the Asp25 carboxyl groups and the position of the O18 hydroxyl hydrogen of DRV are not known, all possible hydrogen bond interactions between the Asp25 carboxyl groups and O18 of the DRV molecules are shown. (A) $DRV_{B\text{-}WT}$ (gray). (B) $DRV_{AE\text{-}WT}$ (blue). (C) $DRV_{B\text{-}D30N/N88D}$ (salmon). (D) $DRV_{AE\text{-}N88S}$ (green).

than the affinities of B-WT protease for NFV and DRV, respectively (Table 2). This result indicates that the AE-WT protease has an inherently weaker affinity for NFV and DRV.

No significant differences in the enthalpy of NFV binding were observed among any of the variants. Although the binding of DRV to all protease variants was enthalpically favorable, the enthalpic contributions were reduced with the AE variants (-10.1 kcal mol^{-1} for AE-WT and -5.1 kcal mol^{-1} for AE-

TABLE 2. Binding thermodynamic parameters for NFV, DRV, and APV binding to AE and clade B variants[a]

Inhibitor and protease variant	K_a (M^{-1})	K_d (nM)	K_d ratio	ΔH (kcal mol^{-1})	$\Delta\Delta H$	$-T\Delta S$ (kcal mol^{-1})	$\Delta(-T\Delta S)$	ΔG (kcal mol^{-1})	$\Delta\Delta G$
NFV									
B-WT	$(2.6 \pm 0.5) \times 10^9$	0.39 ± 0.07	1.0	4.4 ± 0.1		-17.0		-12.6 ± 0.1	
B-D30N/N88D	$(1.2 \pm 0.4) \times 10^8$	8.1 ± 2.8	20.7	6.7 ± 0.3	2.3	-17.5	0.5	-10.8 ± 0.2	1.8
AE-WT	$(3.7 \pm 1.0) \times 10^8$	2.7 ± 0.7	6.9	5.0 ± 0.3	0.6	-16.6	0.9	-11.5 ± 0.2	1.1
AE-N88S	$(5.8 \pm 1.2) \times 10^7$	17.2 ± 3.5	44.1	6.2 ± 0.7	1.8	-16.6	0.9	-10.4 ± 0.1	2.2
DRV									
B-WT	$(2.2 \pm 1.1) \times 10^{11}$	0.004 ± 0.002	1.0	-12.1 ± 0.9		-3.1		-15.2 ± 0.3	
B-D30N/N88D	$(3.7 \pm 0.7) \times 10^{10}$	0.026 ± 0.005	6.5	-12.5 ± 0.4	-0.4	-1.6	1.5	-14.2 ± 0.1	1.0
AE-WT	$(9.1 \pm 0.3) \times 10^{10}$	0.0109 ± 0.0003	2.7	-10.1 ± 0.5	2.0	-4.6	-1.5	-14.7 ± 0.02	0.5
AE-N88S	$(1.1 \pm 0.8) \times 10^{10}$	0.087 ± 0.062	21.8	-5.1 ± 3.6	7.0	-8.4	-5.3	-13.5 ± 0.4	1.7
APV									
B-WT	$(2.6 \pm 1.3) \times 10^9$	0.39 ± 0.20	1.0	-7.3 ± 0.9		-5.3		-12.6 ± 0.3	
B-D30N/N88D	$(1.2 \pm 0.2) \times 10^{10}$	0.08 ± 0.01	0.2	-10.2 ± 1.5	-2.9	-3.3	2.0	-13.5 ± 0.09	-0.9
AE-WT	$(3.1 \pm 0.2) \times 10^9$	0.32 ± 0.02	0.8	-5.5 ± 0.3	-1.8	-7.3	-2.0	-12.70 ± 0.03	-0.1
AE-N88S	$(1.3 \pm 0.9) \times 10^{10}$	0.08 ± 0.06	0.2	-5.0 ± 3.6	2.3	-8.6	-3.3	-13.6 ± 0.4	-1.0

[a] K_a, association constant; K_d, dissociation constant; H, enthalpy; T, temperature; S, entropy; G, Gibbs free energy.

TABLE 3. Enzyme kinetics parameters for clade B and AE-WT and NFV-resistant variants

Parameter	Result for indicated variant			
	B-WT	B-D30N/N88D	AE-WT	AE-N88S
K_m (μM)	16.7 ± 6.0	35.9 ± 0.1	17.5 ± 4.0	19.0 ± 0.8
k_{cat} (s^{-1})	1.79 ± 0.28	0.13 ± 0.09	0.70 ± 0.08	0.20 ± 0.02
k_{cat}/K_m (s^{-1} μM^{-1})	0.11 ± 0.04	0.004 ± 0.002	0.04 ± 0.01	0.010 ± 0.001

TABLE 4. Vitality values for clade B and AE WT and NFV-resistant variants

Inhibitor	Result for indicated variant		
	B-D30N/N88D	AE-WT	AE-N88S
NFV	0.76	2.52	4.01
DRV	0.24	0.99	1.98
APV	0.01	0.30	0.02

N88S) compared with those for the clade B variants (−12.1 kcal mol^{-1} for B-WT and −12.5 kcal mol^{-1} for B-D30N/N88D). As expected, the NFV-resistant variants showed a significant reduction in binding affinity for NFV compared to that of the wild-type variants. With the AE-N88S variant, the affinity for NFV was reduced 44.1-fold (K_d = 17.2 nM) and was far more significant than the D30N/N88D mutations in clade B protease, which reduced the affinity for NFV 20.7-fold (K_d = 8.1 nM). Similarly, the AE-N88S variant had a 21.8-fold-weaker affinity (K_d = 0.087 nM) for DRV compared to a 6.5-fold-weaker affinity (K_d = 0.026 nM) with the B-D30N/N88D variant. Thus, the single N88S substitution in the AE protease has a profound effect on the binding of NFV and DRV.

In contrast to NFV and DRV, clade-specific sequence differences and NFV resistance mutations had only a minimal effect on the affinities for APV of both AE and clade B protease. Despite this, there were some differences in energy parameters. The binding of APV to the clade B variants appeared to be more enthalpically favorable than that to the AE variants. This was compensated for by an increase in the entropic component to the binding energy for the AE proteases.

Protease activity and vitality. The enzyme-kinetic parameters determined for each clade B and AE variant with the CA-p2 fluorogenic substrate analog are summarized in Table 3. The K_m value for B-D30N/N88D protease (35.9 μM) was 2.1-fold greater than that for B-WT protease (16.7 μM). However, the K_m values for the AE protease variants (17.5 μM for AE-WT and 19.0 μM for AE-N88S) were similar to that of B-WT protease. The turnover rate for B-D30N/N88D protease (k_{cat} = 0.13 s^{-1}) was significantly lower than that of B-WT protease (k_{cat} = 1.79 s^{-1}). Turnover rates for AE-WT (k_{cat} = 0.7 s^{-1}) and AE-N88S (k_{cat} = 0.2 s^{-1}) were 2.5 and 8.5-fold lower, respectively, than that of clade B-WT. The k_{cat}/K_m values, or catalytic efficiency values, for B-D30N/N88D and AE variants were lower than that of B-WT protease. Therefore, the reduction in catalytic efficiency of the B-D30N/N88D protease compared with that of B-WT protease resulted from the combined effects of the K_m and k_{cat} values. However, for the AE variants, the lower turnover rates alone were responsible for the reduced catalytic efficiencies. Overall, these results indicate that the polymorphic sequence differences in AE protease can alter the activity profile of the enzyme compared to results with the clade B protease.

Vitality values were calculated to determine if the protease variants had a selective advantage over NFV, DRV, and APV. AE-WT and AE-N88S protease had calculated vitality values of 2.52 and 4.01 for NFV, respectively, compared with 0.76 for B-WT (Table 4). However, vitality values for DRV were not significantly different from that of B-WT protease. Vitality values for APV were significantly lower for all variants than for B-WT protease. These results indicate that AE-WT may have a selective advantage over NFV compared to B-WT but that the AE variants may not have a significant selective advantage against DRV or APV relative to B-WT.

DISCUSSION

Although the majority of HIV-1 patients are infected with non-B forms of the virus, molecular studies have been carried out predominantly with clade B variants. The AE protease has several polymorphisms that are associated with inhibitor resistance in clade B. AE also shows altered patterns of drug resistance to NFV. We have performed detailed studies to determine the effects of sequence polymorphisms on enzyme structure, activity, and inhibitor binding. These analyses led to a structural rationalization for the altered pathways for drug resistance.

AE-WT protease has an inherently weaker affinity for NFV and DRV than that of B-WT, as is evident from the thermodynamic data (Table 2). The weaker affinity observed for NFV is consistent with previously published data for another AE protease variant (3), as well as for clade A protease (42), which is closely related. The inherent weaker affinity for NFV likely allows the AE protease to gain resistance to NFV through a single nonactive-site substitution, N88S. The clade B protease, in contrast, which has a relatively stronger affinity for NFV, requires a combination of an active-site mutation (D30N) and a nonactive-site mutation (N88D) to gain NFV resistance. The ability of the AE-N88S protease to maintain affinity for substrates is evident from our enzyme kinetics data (Table 4), in which the K_m value for AE-N88S was comparable to that of AE-WT and B-WT protease. The K_m value for clade B-D30N/N88D, on the other hand, was significantly worse than that of the B-WT, likely reflecting the effect of the altered active site.

As an active-site residue, Asp30 plays a key role in substrate recognition by interacting with substrates through side chain-mediated hydrogen bonds with the MA-CA, CA-p2, p1-p6, and p2-NC cleavage sites (36). Therefore, as is evident from our enzyme kinetics data, the D30N/N88D mutations in clade B will likely affect substrate binding and processing. Several studies have observed substrate coevolution in instances in which the protease mutates active-site residues in order to confer inhibitor resistance (22, 23). However, since the AE-N88S protease variant has no active-site mutations, the enzyme retains the ability to effectively recognize substrates while conferring NFV resistance. Therefore, the presence of the N88S substitution in AE protease is unlikely to induce coevolution of

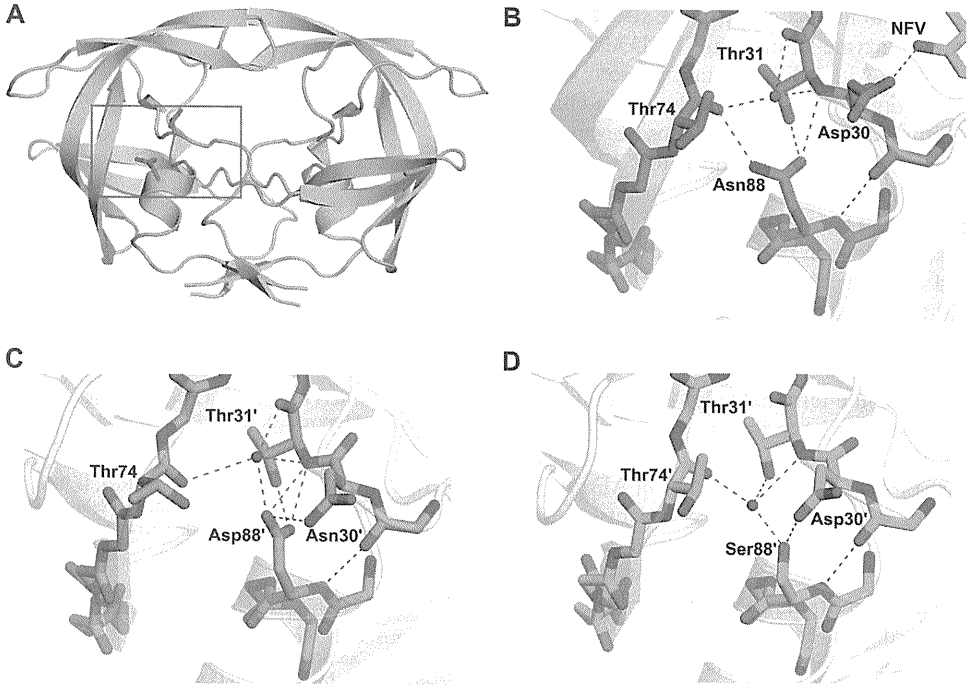

FIG. 4. Hydrogen bond network involving residue 88. (A) Asn88 bridges the terminal helix with Asp30 from the active site and Thr74 from one of the outer beta strands. The red box indicates the region of the protease molecule highlighted in panels B to D. (B) Asn88 in $NFV_{B\text{-}WT}$ (PDB code 3EKX). (C) Asp88 in $DRV_{B\text{-}D30N/N88D}$. (D) Ser88 in $DRV_{N88S\text{-}WT}$. Hydrogen bond interactions are indicated by red dashed lines.

the viral substrates in order to maintain effective enzymatic activity.

Despite having K_m values that were comparable to that of B-WT protease, both AE-WT and AE-N88S had significantly lower catalytic turnover rates (k_{cat}) than that of the B-WT protease (Table 3). As a result, the catalytic efficiency of the AE variants is lower than that of the B-WT protease. The lower turnover rates of the AE variants could be a direct result of the reduced flexibility of the flap hinge (residues 33 to 39) and core regions (residues 16 to 22) of the protein. Molecular dynamics studies have revealed that hydrophobic sliding of the core region facilitates substrate binding through the opening of the active site (9). The unique hydrogen bonds observed between the flap hinge and the core in the AE variants alter movement of the core, thus impacting the ability of the active site to open up for substrate binding and product release. Based on our enzyme kinetics data, this altered flexibility of the flap hinges in the AE variants has little effect on substrate binding but rather affects the catalytic step of the reaction by slowing down product release.

The higher vitality value observed for AE-WT with NFV provides supporting evidence for the reduction in the efficacy of NFV against the AE protease compared with that of clade B (Table 4). This result is consistent with previous vitality calculations for the clade A protease (42). In addition, these results further highlight the idea that background polymorphic sequence variations in the AE protease can affect the potency of NFV. The suboptimal efficacy of NFV against the AE-WT protease likely permits a nonactive-site variant, AE-N88S, to emerge over variants with active-site mutations to effectively confer resistance to NFV.

The impact on other inhibitors, however, is complex. APV and DRV are chemically very closely related compounds, and similar susceptibility and resistance patterns have been observed for these two inhibitors (31). However, this pattern is not evident for this series of resistant variants. Both the N88S mutation in the AE and the D30N/N88D mutations in the clade B proteases result in hypersusceptibility to APV. Similar results have been observed also for a B-N88S protease variant (24, 45). In contrast, the same substitutions in the protease give rise to even greater resistance to DRV. However, since DRV presents a greater genetic barrier to resistance than APV (33), the *in vivo* implications of weaker affinity for DRV in the AE variants are likely negligible. Indeed, our calculated vitality values indicate that DRV maintains its potency against the AE variants despite having a weaker affinity for AE-WT and AE-N88S relative to clade B protease.

A close look at the $NFV_{B\text{-}WT}$ protease complex reveals an important interaction between the Asp30 residue side chain and the inhibitor bound in the active site. (PDB code 3EKX) (Fig. 4A and B). One of the side chain oxygen atoms of Asp30 forms a direct hydrogen bond with the O38 atom of NFV. Our crystal structures of the NFV-resistant variants show that N88S in AE and N88D in clade B have the ability to interact with residue 30 and orient it away from the active site (Fig. 3B and D) and thereby disrupt the interaction between residue 30 and the inhibitor. These structural observations are similar to interpretations made in previous molecular dynamics studies involving NFV-protease complexes (27, 28). Thus, NFV resistance is likely caused in large part due to the loss of this interaction in the NFV-resistant variants.

Overall, mutations that emerge in response to inhibitor ther-

apy need to have a minimal impact on protease structure and activity to maintain the enzyme's function. The D30N substitution, which is associated with NFV resistance, is one of the few drug-resistant mutations that involve a change in charge. The additional substitution of N88D likely helps preserve the net charge on the protein. In AE, resistance to NFV occurs indirectly with the N88S mutation. Likewise, the sole NFV-resistant alteration, N88S, in the AE protease does not change the overall electrostatics. Thus, in both clade B and AE, NFV resistance is attained with no change to the net charge of the enzyme. In the wild-type variants, Asn88 is one of the few internal hydrogen bonding side chains in the core of the protease monomer. The side chain of Asn88 has a key role in the protease structure bridging the terminal helix, with residues 30 and 31 coming from the active site to the backbone of Thr74 in the center of one of the outer beta strands (Fig. 4A and B). With the substitutions of Asp in clade B and Ser in AE for Asn at position 88 in the NFV-resistant protease variants, the hydrogen bonding network is preserved through the coordination of some key water molecules in the core of the protease monomer (Fig. 4B to D). Thus, mutations confer resistance to NFV through a series of interdependent changes that preserve the structural and electrostatic properties of HIV-1 protease.

In conclusion, protease activity and the response to protease inhibitors can be affected by clade-specific sequence differences. Our findings likely extend beyond HIV-1 protease to other drug targets within HIV and underscore the need to consider clade-specific polymorphisms when developing new drugs and formulating treatment plans. Furthermore, drug resistance pathways observed in the context of clade B viruses cannot be assumed to hold true for other HIV-1 clades.

ACKNOWLEDGMENTS

This work was supported by grants from the National Institutes of Health (P01-GM66524) and Tibotec, Inc., to C.A.S. Additionally, this study was supported by a Grant-in-Aid for AIDS research from the Ministry of Health, Labor, and Welfare of Japan (H19-AIDS-007) to W.S.

We thank William Royer, Moses Prabu-Jayabalan, and Madhavi Nalam for helpful discussions and Christina Ng and Brendan Hilbert for assistance with data collection.

We gratefully acknowledge the Mail-In Data Collection Program of the National Synchrotron Light Source, Brookhaven National Laboratory, for collecting X-ray data at the X29A beamline, for which financial support comes principally from the Offices of Biological and Environmental Research and of Basic Energy Sciences of the U.S. Department of Energy and from the National Center for Research Resources of the National Institutes of Health. Use of the Advanced Photon Source for X-ray data collection was supported by the U.S. Department of Energy, Basic Energy Sciences, Office of Science, under contract DE-AC02-06CH11357. Use of the BioCARS Sector 14 was supported by the National Institutes of Health, National Center for Research Resources, under grant RR007707.

The protease inhibitors used in this study were obtained through the NIH AIDS Research and Reference Reagent Program, Division of AIDS, National Institute of Allergy and Infectious Diseases, NIH.

REFERENCES

1. **Ariyoshi, K., M. Matsuda, H. Miura, S. Tateishi, K. Yamada, and W. Sugiura.** 2003. Patterns of point mutations associated with antiretroviral drug treatment failure in CRF01_AE (subtype E) infection differ from subtype B infection. J. Acquir. Immune Defic. Syndr. **33:**336–342.
2. **Carr, J. K., M. O. Salminen, C. Koch, D. Gotte, A. W. Artenstein, P. A. Hegerich, D. St. Louis, D. S. Burke, and F. E. McCutchan.** 1996. Full-length sequence and mosaic structure of a human immunodeficiency virus type 1 isolate from Thailand. J. Virol. **70:**5935–5943.
3. **Clemente, J. C., R. M. Coman, M. M. Thiaville, L. K. Janka, J. A. Jeung, S. Nukoolkarn, L. Govindasamy, M. Agbandje-McKenna, R. McKenna, W. Leelamanit, M. M. Goodenow, and B. M. Dunn.** 2006. Analysis of HIV-1 CRF_01 A/E protease inhibitor resistance: structural determinants for maintaining sensitivity and developing resistance to atazanavir. Biochemistry **45:** 5468–5477.
4. **Collaborative Computational Project, Number 4.** 1994. The CCP4 suite: programs for protein crystallography. Acta Crystallogr. D Biol. Crystallogr. **50:**760–763.
5. **Copeland, R. A.** 1996. Enzymes: a practical introduction to structure, mechanism, and data analysis. Wiley-VCH, New York, NY.
6. **DeLano, W. L.** 2002. The PyMol molecular graphics system. DeLano Scientific, San Carlos, CA.
7. **de Oliveira, T., S. Engelbrecht, E. Janse van Rensburg, M. Gordon, K. Bishop, J. zur Megede, S. W. Barnett, and S. Cassol.** 2003. Variability at human immunodeficiency virus type 1 subtype C protease cleavage sites: an indication of viral fitness? J. Virol. **77:**9422–9430.
8. **Emsley, P., and K. Cowtan.** 2004. Coot: model-building tools for molecular graphics. Acta Crystallogr. D Biol. Crystallogr. **60:**2126–2132.
9. **Foulkes-Murzycki, J. E., W. R. Scott, and C. A. Schiffer.** 2007. Hydrophobic sliding: a possible mechanism for drug resistance in human immunodeficiency virus type 1 protease. Structure **15:**225–233.
10. **Gao, F., D. L. Robertson, S. G. Morrison, H. Hui, S. Craig, J. Decker, P. N. Fultz, M. Girard, G. M. Shaw, B. H. Hahn, and P. M. Sharp.** 1996. The heterosexual human immunodeficiency virus type 1 epidemic in Thailand is caused by an intersubtype (A/E) recombinant of African origin. J. Virol. **70:**7013–7029.
11. **Geretti, A. M.** 2006. HIV-1 subtypes: epidemiology and significance for HIV management. Curr. Opin. Infect. Dis. **19:**1–7.
12. **Gomes, P., I. Diogo, M. F. Gonçalves, P. Carvalho, J. Cabanas, M. C. Lobo, and R. Camacho.** 2002. Different pathways to nelfinavir genotypic resistance in HIV-1 subtypes B and G. Conference on Retroviruses and Opportunistic Infections, abstract 46. Conference on Retroviruses and Opportunistic Infections, Seattle, WA.
13. **Grossman, Z., E. E. Paxinos, D. Averbuch, S. Maayan, N. T. Parkin, D. Engelhard, M. Lorber, V. Istomin, Y. Shaked, E. Mendelson, D. Ram, C. J. Petropoulos, and J. M. Schapiro.** 2004. Mutation D30N is not preferentially selected by human immunodeficiency virus type 1 subtype C in the development of resistance to nelfinavir. Antimicrob. Agents Chemother. **48:**2159–2165.
14. **Gulnik, S. V., L. I. Suvorov, B. Liu, B. Yu, B. Anderson, H. Mitsuya, and J. W. Erickson.** 1995. Kinetic characterization and cross-resistance patterns of HIV-1 protease mutants selected under drug pressure. Biochemistry **34:** 9282–9287.
15. **Hemelaar, J., E. Gouws, P. D. Ghys, and S. Osmanov.** 2006. Global and regional distribution of HIV-1 genetic subtypes and recombinants in 2004. AIDS **20:**W13–23.
16. **Hu, D. J., A. Buve, J. Baggs, G. van der Groen, and T. J. Dondero.** 1999. What role does HIV-1 subtype play in transmission and pathogenesis?: an epidemiological perspective. AIDS **13:**873–881.
17. **Kaleebu, P., N. French, C. Mahe, D. Yirrell, C. Watera, F. Lyagoba, J. Nakiyingi, A. Rutebemberwa, D. Morgan, J. Weber, C. Gilks, and J. Whitworth.** 2002. Effect of human immunodeficiency virus (HIV) type 1 envelope subtypes A and D on disease progression in a large cohort of HIV-1-positive persons in Uganda. J. Infect. Dis. **185:**1244–1250.
18. **Kanki, P. J., D. J. Hamel, J. L. Sankale, C. Hsieh, I. Thior, F. Barin, S. A. Woodcock, A. Gueye-Ndiaye, E. Zhang, M. Montano, T. Siby, R. Marlink, I. NDoi, M. E. Essex, and S. MBoup.** 1999. Human immunodeficiency virus type 1 subtypes differ in disease progression. J. Infect. Dis. **179:**68–73.
19. **Kantor, R., D. A. Katzenstein, B. Efron, A. P. Carvalho, B. Wynhoven, P. Cane, J. Clarke, S. Sirivichayakul, M. A. Soares, J. Snoeck, C. Pillay, H. Rudich, R. Rodrigues, A. Holguin, K. Ariyoshi, M. B. Bouzas, P. Cahn, W. Sugiura, V. Soriano, L. F. Brigido, Z. Grossman, L. Morris, A. M. Vandamme, A. Tanuri, P. Phanuphak, J. N. Weber, D. Pillay, P. R. Harrigan, R. Camacho, J. M. Schapiro, and R. W. Shafer.** 2005. Impact of HIV-1 subtype and antiretroviral therapy on protease and reverse transcriptase genotype: results of a global collaboration. PLoS Med. **2:**e112.
20. **King, N. M., L. Melnick, M. Prabu-Jeyabalan, E. A. Nalivaika, S.-S. Yang, Y. Gao, X. Nie, C. Zepp, D. L. Heefner, and C. A. Schiffer.** 2002. Lack of synergy for inhibitors targeting a multi-drug-resistant HIV-1 protease. Protein Sci. **11:**418–429.
21. **King, N. M., M. Prabu-Jeyabalan, P. Wigerinck, M.-P. de Béthune, and C. A. Schiffer.** 2004. Structural and thermodynamic basis for the binding of TMC114, a next-generation human immunodeficiency virus type 1 protease inhibitor. J. Virol. **78:**12012–12021.
22. **Kolli, M., S. Lastere, and C. A. Schiffer.** 2006. Co-evolution of nelfinavir-resistant HIV-1 protease and the p1-p6 substrate. Virology **347:**405–409.
23. **Kolli, M., E. Stawiski, C. Chappey, and C. A. Schiffer.** 2009. Human immunodeficiency virus type 1 protease-correlated cleavage site mutations enhance inhibitor resistance. J. Virol. **83:**11027–11042.
24. **Masquelier, B., K. L. Assoumou, D. Descamps, L. Bocket, J. Cottalorda, A. Ruffault, A. G. Marcelin, L. Morand-Joubert, C. Tamalet, C. Charpentier,**

G. Peytavin, Z. Antoun, F. Brun-Vezinet, and D. Costagliola. 2008. Clinically validated mutation scores for HIV-1 resistance to fosamprenavir/ritonavir. J. Antimicrob. Chemother. **61:**1362–1368.

25. **Murphy, E., B. Korber, M. C. Georges-Courbot, B. You, A. Pinter, D. Cook, M. P. Kieny, A. Georges, C. Mathiot, F. Barre-Sinoussi, et al.** 1993. Diversity of V3 region sequences of human immunodeficiency viruses type 1 from the Central African Republic. AIDS Res. Hum. Retroviruses **9:**997–1006.
26. **Nunez, M., C. de Mendoza, L. Valer, E. Casas, S. Lopez-Calvo, A. Castro, B. Roson, D. Podzamczer, A. Rubio, J. Berenguer, and V. Soriano.** 2002. Resistance mutations in HIV-infected patients experiencing early failure with nelfinavir-containing triple combinations. Med. Sci. Monit **8:**CR620–CR623.
27. **Ode, H., S. Matsuyama, M. Hata, T. Hoshino, J. Kakizawa, and W. Sugiura.** 2007. Mechanism of drug resistance due to N88S in CRF01_AE HIV-1 protease, analyzed by molecular dynamics simulations. J. Med. Chem. **50:** 1768–1777.
28. **Ode, H., M. Ota, S. Neya, M. Hata, W. Sugiura, and T. Hoshino.** 2005. Resistant mechanism against nelfinavir of human immunodeficiency virus type 1 proteases. J. Phys. Chem. B **109:**565–574.
29. **Otwinowski, Z., and W. Minor.** 1997. Processing of X-ray diffraction data collected in oscillation mode. Methods Enzymol. **276:**307–326.
30. **Painter, J., and E. A. Merritt.** 2006. Optimal description of a protein structure in terms of multiple groups undergoing TLS motion. Acta Crystallogr. D Biol. Crystallogr. **62:**439–450.
31. **Parkin, N., E. Stawiski, C. Chappey, and E. Coakley.** 2007. Darunavir/amprenavir cross-resistance in clinical samples submitted for phenotype/genotype combination resistance testing. Conference on Retroviruses and Opportunistic Infections, abstract 607. Conference on Retroviruses and Opportunistic Infections, San Francisco, CA.
32. **Plantier, J. C., M. Leoz, J. E. Dickerson, F. De Oliveira, F. Cordonnier, V. Lemee, F. Damond, D. L. Robertson, and F. Simon.** 2009. A new human immunodeficiency virus derived from gorillas. Nat. Med. **15:**871–872.
33. **Poveda, E., C. de Mendoza, L. Martin-Carbonero, A. Corral, V. Briz, J. Gonzalez-Lahoz, and V. Soriano.** 2007. Prevalence of darunavir resistance mutations in HIV-1-infected patients failing other protease inhibitors. J. Antimicrob. Chemother. **60:**885–888.
34. **Prabu-Jeyabalan, M., E. Nalivaika, N. M. King, and C. A. Schiffer.** 2004. Structural basis for coevolution of the human immunodeficiency virus type 1 nucleocapsid-p1 cleavage site with a V82A drug-resistant mutation in viral protease. J. Virol. **78:**12446–12454.
35. **Prabu-Jeyabalan, M., E. A. Nalivaika, K. Romano, and C. A. Schiffer.** 2006. Mechanism of substrate recognition by drug-resistant human immunodeficiency virus type 1 protease variants revealed by a novel structural intermediate. J. Virol. **80:**3607–3616.
36. **Prabu-Jeyabalan, M., E. A. Nalivaika, and C. A. Schiffer.** 2002. Substrate shape determines specificity of recognition for HIV-1 protease: analysis of crystal structures of six substrate complexes. Structure **10:**369–381.
37. **Robertson, D. L., J. P. Anderson, J. A. Bradac, J. K. Carr, B. Foley, R. K. Funkhouser, F. Gao, B. H. Hahn, M. L. Kalish, C. Kuiken, G. H. Learn, T. Leitner, F. McCutchan, S. Osmanov, M. Peeters, D. Pieniazek, M. Salminen, P. M. Sharp, S. Wolinsky, and B. Korber.** 2000. HIV-1 nomenclature proposal. Science **288:**55–56.
38. **Rose, J. R., R. Salto, and C. S. Craik.** 1993. Regulation of autoproteolysis of the HIV-1 and HIV-2 proteases with engineered amino acid substitutions. J. Biol. Chem. **268:**11939–11945.
39. **Spira, S., M. A. Wainberg, H. Loemba, D. Turner, and B. G. Brenner.** 2003. Impact of clade diversity on HIV-1 virulence, antiretroviral drug sensitivity and drug resistance. J. Antimicrob. Chemother. **51:**229–240.
40. **Surleraux, D. L., A. Tahri, W. G. Verschueren, G. M. Pille, H. A. de Kock, T. H. Jonckers, A. Peeters, S. De Meyer, H. Azijn, R. Pauwels, M. P. de Bethune, N. M. King, M. Prabu-Jeyabalan, C. A. Schiffer, and P. B. Wigerinck.** 2005. Discovery and selection of TMC114, a next generation HIV-1 protease inhibitor. J. Med. Chem. **48:**1813–1822.
41. **Tebit, D. M., I. Nankya, E. J. Arts, and Y. Gao.** 2007. HIV diversity, recombination and disease progression: how does fitness "fit" into the puzzle? AIDS Rev. **9:**75–87.
42. **Velazquez-Campoy, A., M. J. Todd, S. Vega, and E. Freire.** 2001. Catalytic efficiency and vitality of HIV-1 proteases from African viral subtypes. Proc. Natl. Acad. Sci. U. S. A. **98:**6062–6067.
43. **Velazquez-Campoy, A., S. Vega, E. Fleming, U. Bacha, Y. Sayed, H. W. Dirr, and E. Freire.** 2003. Protease inhibition in African subtypes of HIV-1. AIDS Rev. **5:**165–171.
44. **Williams, T., and C. Kelley.** Accessed 28 January 2009. gnuplot, version 4.2. http://www.gnuplot.info/.
45. **Ziermann, R., K. Limoli, K. Das, E. Arnold, C. J. Petropoulos, and N. T. Parkin.** 2000. A mutation in human immunodeficiency virus type 1 protease, N88S, that causes in vitro hypersensitivity to amprenavir. J. Virol. **74:**4414–4419.

5356 J. Med. Chem. 2010, 53, 5356–5360
DOI: 10.1021/jm1003528

Journal of Medicinal Chemistry
Brief Article

Peptide HIV-1 Integrase Inhibitors from HIV-1 Gene Products

Shintaro Suzuki,[†,#] Emiko Urano,[‡,#] Chie Hashimoto,[†] Hiroshi Tsutsumi,[†] Toru Nakahara,[†] Tomohiro Tanaka,[†] Yuta Nakanishi,[†] Kasthuraiah Maddali,[§] Yan Han,[‡] Makiko Hamatake,[‡] Kosuke Miyauchi,[‡] Yves Pommier,[§] John A. Beutler,[⊥] Wataru Sugiura,[‡] Hideyoshi Fuji,[∥] Tyuji Hoshino,[∥] Kyoko Itotani,[†] Wataru Nomura,[†] Tetsuo Narumi,[†] Naoki Yamamoto,[‡] Jun A. Komano,[‡] and Hirokazu Tamamura*[,†]

[†]*Department of Medicinal Chemistry, Institute of Biomaterials and Bioengineering, Tokyo Medical and Dental University, 2-3-10 Kandasurugadai, Chiyoda-ku, Tokyo 101-0062, Japan,* [‡]*AIDS Research Center, National Institute of Infectious Diseases, 1-23-1 Toyama, Shinjuku-ku, Tokyo 162-8640, Japan,* [§]*Laboratory of Molecular Pharmacology, Center for Cancer Research, National Cancer Institute, National Institutes of Health, Bethesda, Maryland 20892-4255,* [∥]*Department of Physical Chemistry, Graduate School of Pharmaceutical Sciences, Chiba University, 1-33 Yayoi-cho, Inage-ku, Chiba 263-8522, Japan, and* [⊥]*Molecular Targets Laboratory, Center for Cancer Research, National Cancer Institute, National Institutes of Health, Frederick, Maryland 21702.* [#] *These authors contributed equally to this work.*

Received March 17, 2010

Anti-HIV peptides with inhibitory activity against HIV-1 integrase (IN) have been found in overlapping peptide libraries derived from HIV-1 gene products. In a strand transfer assay using IN, inhibitory active peptides with certain sequential motifs related to Vpr- and Env-derived peptides were found. The addition of an octa-arginyl group to the inhibitory peptides caused a remarkable inhibition of the strand transfer and 3′-end-processing reactions catalyzed by IN and significant inhibition against HIV replication.

Introduction

Many antiretroviral drugs are currently available to treat human immunodeficiency virus type 1 (HIV-1) infection. Viral enzymes such as reverse transcriptase (RT[a]), protease and integrase (IN), gp41, and coreceptors are the main targets for antiretroviral drugs that are under development. Because of the emergence of viral strains with multidrug resistance (MDR), however, new anti-HIV-1 drugs operating with different inhibitory mechanisms are required. Following the success of raltegravir, IN has emerged as a prime target. IN is an essential enzyme for the stable infection of host cells because it catalyzes the insertion of viral DNA inside the preintegration complex (PIC) into the genome of host cells in two successive reactions, designated as strand transfer and 3′-end-processing. It is assumed that the enzymatic activities of IN have to be negatively regulated in the PIC during its transfer from the cytoplasm to the nucleus. Otherwise, premature activation of IN can lead to the autointegration into the viral DNA itself, resulting in an aborted infection. We speculate that the virus, rather than the host cells, must encode a mechanism to prevent autointegration. The PIC contains in association with the viral nucleic acid, viral proteins such as RT, IN, capsids ($p24^{CA}$ and $p7^{NC}$), matrix ($p17^{MA}$), p6 and Vpr, cellular proteins HMG I (Y), and the barrier to autointegration factor (BAF).[1−4] It is likely that, due to their spatial proximity in the PIC, these proteins physically and functionally interact with each other. For instance, it is already known that RT activity inhibited by Vpr,[5] and that RT and IN inhibit each other.[5−9] Vpr also inhibits IN through its C-terminal domain.[5,10] Because these studies suggest that PIC components regulate each other's function, we have attempted to obtain potent inhibitory lead compounds from a peptide fragment library derived from HIV-1 gene products, an approach which has been successful in finding a peptide IN inhibitor from LEDGF, a cellular IN binding protein.[11]

In this paper, we describe the screening of an overlapping peptide library derived from HIV-1 proteins, the identification of certain peptide motifs with inhibitory activity against HIV-1 IN, and the evaluation of effective inhibition of HIV-1 replication in cells using the identified peptide inhibitors possessing cell membrane permeability.

Results and Discussion

An overlapping peptide library spanning HIV-1 SF2 *Gag*, *Pol*, *Vpr*, *Tat*, *Rev*, *Vpu*, *Env*, and *Nef*, provided by Dr. Iwamoto of the Institute of Medical Science at the University of Tokyo (Supporting Information, SI, Figure 2A), was screened with a strand transfer assay[12] in search of peptide pools with inhibitory activity against HIV-1 IN. The library consists of 658 peptide fragments derived from the HIV-1 gene products. Each peptide is composed of 10−17 amino acid residues with overlapping regions of 1−7 amino acid residues. Sixteen peptide pools containing between 16 and 65 peptides were used for the first screening at the final concentration of 5.0 μM for each peptide (SI Figure 2B). This initial screening gave the results shown in Figure 1. Both Vpr and Env4 pools showed remarkable inhibition of IN strand transfer activity, and consequently a second screening was performed using the individual peptides contained in the Vpr and Env4 pools. A group of consecutive overlapping peptides in the Vpr pool (groups 13−15) and groups 4−6 and 20−21 in the Env4 pool were found to possess IN inhibitory activity (Figure 2). We focused on Vpr15 and Env4-4 peptides because they showed inhibitory activity against IN strand transfer reaction in a dose-dependent manner (Figure 3). The IC_{50} values of Vpr15

*To whom correspondence should be addressed. Phone: +81-3-5280-8036. Fax: +81-3-5280-8039. E-mail: tamamura.mr@tmd.ac.jp.

[a]Abbreviations: HIV, human immunodeficiency virus; IN, integrase; RT, reverse transcriptase; MDR, multidrug resistance; PIC, preintegration complex; BAF, barrier to autointegration factor; R_8, octa-arginyl.

pubs.acs.org/jmc Published on Web 06/29/2010

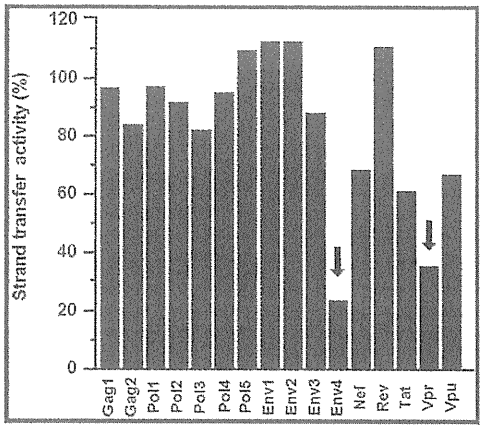

Figure 1. Inhibition of the IN strand transfer activity by peptide pools. Inhibition of the IN strand transfer activity was strongly inhibited by Env4 and Vpr pools (arrows). The *y*-axis represents the IN strand transfer activity relative to the solvent control (DMSO).

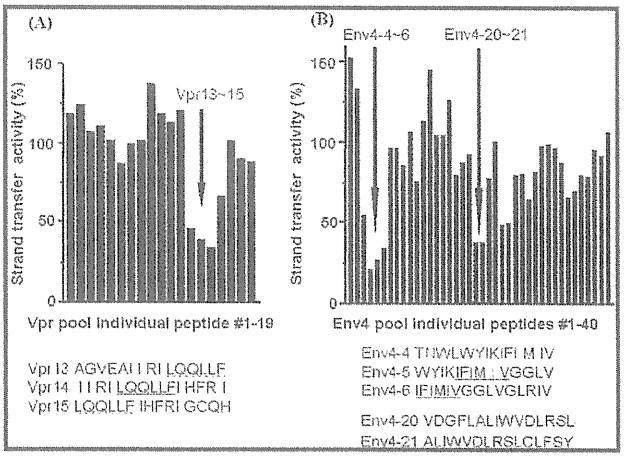

Figure 2. Identification of IN inhibitory peptides in the Vpr (A) and Env4 (B) pools based on the strand transfer activity of IN. The consecutive overlapping peptides display the inhibition of the strand transfer activity of IN (arrows). The *y*-axis represents the IN strand transfer activity relative to the solvent control (DMSO). The concentration of each peptide was 5 μM. The common sequences of individual peptides derived from Vpr and Env4 pools with anti-IN activity are underlined.

and Env4-4 were estimated at 5.5 and 1.9 μM, respectively. These peptides did not show any significant inhibitory activity against HIV-1 RT, suggesting that they might inhibit IN strand transfer reaction selectively.

The overlapping peptides of Vpr13-15 and Env4-4-6 have the vommon hexapeptide sequences LQQLLF and IFIMIV, respectively. The LQQLLF sequence covers positions 64−69 of Vpr, which is a part of the second helix of Vpr. The IFIMIV sequence corresponds to positions 684−689 of gp160, which is a part of the transmembrane domain of TM gp41. These hexapeptides are thought to be critical to inhibition of IN activity. It was recently reported[5] that similar peptides derived from Vpr inhibit IN with IC_{50} values of 1−16 μM, which is consistent with our data. In this report,[5] the peptide motif was found to be 15 amino acid residues spanning LQQLLF from the overlapping Vpr peptide library. In our study, more precise mapping of inhibitory motif in Vpr peptides was achieved by identifying the shorter effective peptide motif. We focused on the Vpr-derived peptide, LQQLLF (Vpr-1) to develop potent inhibitory peptides. However, the expression of inhibitory activity against IN

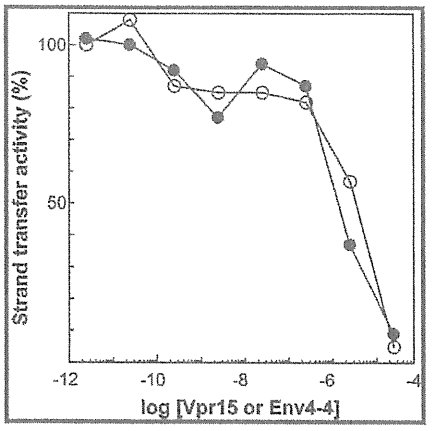

Figure 3. Concentration-dependent inhibition of IN strand transfer activities by Vpr15 (○) and Env4−4 (●) peptides. The *y*-axis represents the IN strand transfer activity relative to the solvent control (DMSO).

in vivo by only hexapeptides might be difficult because these hexapeptides penetrate the plasma membrane very poorly and to achieve antiviral activity, it is essential that they penetrate the cell membrane. To that effect, an octa-arginyl (R_8) group[13] was fused to the Vpr-derived peptides (Table 1). R_8 is a cell membrane permeable motif and its fusion with parent peptides successfully generates bioactive peptides without significant adverse effects or cytotoxicity.[14−18] In addition, the R_8-fusion could increase the solubility of Vpr-derived peptides which have a relatively hydrophobic character.

The inhibitory activity of Vpr-1 and Vpr-1-4 R_8 peptides against IN was evaluated based on the strand transfer and 3′-end-processing reactions in vitro (Table 1).[19,20] Vpr-1 did not show strong inhibition of either IN activity, but the IC_{50} of Vpr-1 R_8 toward the strand transfer reaction of IN was 10-fold lower than that of Vpr-1 lacking the R_8 group. This indicates that the positive charges derived from the R_8 group might enhance the inhibitory activity of the Vpr-1 peptide. Because we were concerned that the strong positive charges close to the LQQLLF motif might interfere with the inhibitory activity, the 6 amino acid sequence (−IHFRIG−) was inserted as a spacer between LQQLLF and R_8 (Vpr-3 R_8). The IHFRIG sequence was used to reconstitute the natural Vpr. The IC_{50} values of Vpr-2 R_8 for the strand transfer and 3′-end-processing activities of IN were 0.70 and 0.83 μM, respectively, while Vpr-3 R_8 showed potent IN inhibitory activities of 4.0 and 8.0 nM against the strand transfer and 3′-end- processing activities, respectively. This result indicates the additional importance of the IHFRIG sequence for inhibitory activities against IN. The increased IN inhibitory activities might be achieved presumably by the synergistic effect of the LQQLLF motif, the IHFRIG sequence, and the R_8 group. Vpr-4 R_8, in which the EAIIRI sequence was attached to further reconstitute the Vpr helix 2, showed inhibitory activities similar to those of Vpr-3 R_8, suggesting that reconstitution of helix 2 of Vpr is not necessary for efficient IN inhibition. Vpr-3 R_8 and Vpr-4 R_8, with $IC_{50} > 0.5$ μM,[21] were less potent inhibitors of RT-associated RNase H activity, indicating that these peptides can selectively inhibit IN. These results suggest that Vpr-derived peptides are novel and distinct from any other IN inhibitors reported to date.

For rapid assessment of the antiviral effect of Vpr-derived peptides, we established an MT-4 Luc system in which MT-4 cells were stably transduced with the firefly luciferase expression cassette by a murine leukemia viral vector (SI Figure 3).

Table 1. Sequences of Vpr-Derived Peptides and Their IC_{50} Values toward the Strand Transfer and 3′-End Processing Reactions of IN

	sequence	IC_{50} (μM) strand transfer	3′-end processing
Vpr-1	LQQLLF	68 ± 1.0	> 100
Vpr-1 R_8	Ac-LQQLLF-RRRRRRRR-NH_2	6.1 ± 1.1	> 11
Vpr-2 R_8	Ac-IHFRIG-RRRRRRRR-NH_2	0.70 ± 0.06	0.83 ± 0.07
Vpr-3 R_8	Ac-LQQLLF IHFRIG-RRRRRRRR-NH_2	0.004 ± 0.0001	0.008 ± 0.001
Vpr-4 R_8	Ac-EAIIRI LQQLLF IHFRIG-RRRRRRRR-NH_2	0.005 ± 0.002	0.006 ± 0.006

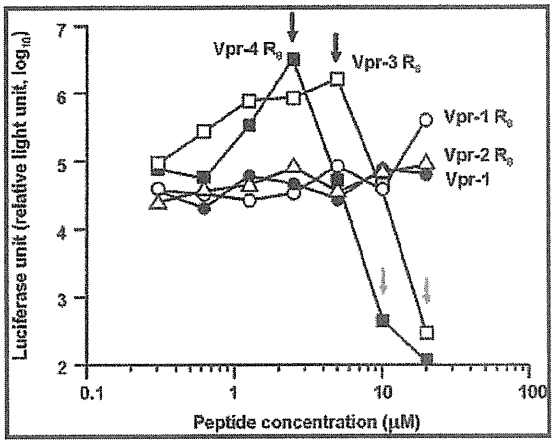

Figure 4. Luciferase signals in MT-4 Luc cells infected with HIV-1 in the presence of various concentrations of Vpr-derived peptides: Vpr-1 (●), Vpr-1 R_8 (○), Vpr-2 R_8 (△), Vpr-3 R_8 (□), Vpr-4 R_8 (■).

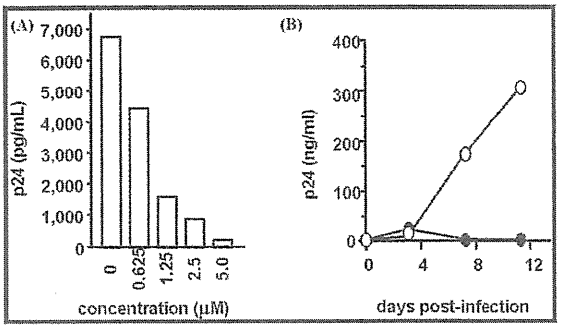

Figure 5. (A) The inhibition of HIV-$1_{JR\text{-}CSF}$ replication in NP2-CD4-CCR5 cells in the presence of various concentrations of Vpr-3 R_8. (B) The replication kinetics of HIV-1_{HXB2} in MT-4 cells in the presence of Vpr-3 R_8 (●). The concentration of Vpr-3 R_8 was fixed at 0.5 μM. Absence of Vpr-3 R_8 (○).

MT-4 Luc cells constitutively express high levels of luciferase which are significantly reduced by HIV-1 infection due to their high susceptibility to cell death upon HIV-1 infection. Protection of MT-4 Luc cells from HIV-1-induced cell death maintains the luciferase signals at high levels. In addition, the cytotoxicity of Vpr-derived peptides can be evaluated by a decrease of luciferase signals in these MT-4 Luc systems. Vpr-2 R_8, which is a weak IN inhibitor, showed no significant anti-HIV-1 activity below concentrations of 20 μM, suggesting that its moderate IC_{50} level in vitro is not sufficient to suppress HIV-1 replication in tissue culture and that the R_8 group is not significantly cytotoxic (Figure 4). Vpr-1 did not show any inhibitory effects against HIV-1 replication; however, Vpr-1 R_8 displayed a weak antiviral effect at a concentration of 20 μM and both Vpr-3 R_8 and Vpr-4 R_8 showed significant inhibitory effects against HIV-1 replication. The R_8 peptide did not show significant anti-HIV activity (IC_{50} > 50 μM, data not shown). These results suggest that the addition of the R_8 group enables Vpr-derived peptides to enter the cytoplasm and access IN, with the result that HIV-1 replication could be effectively inhibited.

Because Vpr-3 R_8 was less cytotoxic than Vpr-4 R_8, the inhibitory activities of Vpr-3 R_8 were further investigated. Two replication assay systems, R5-tropic HIV-$1_{JR\text{-}CSF}$ on NP2-CD4-CCR5 cells and X4-tropic HIV-1_{HXB2} on MT-4 cells, were utilized. NP2-CD4-CCR5 cells were infected with HIV-$1_{JR\text{-}CSF}$ in the presence of various concentrations of Vpr-3 R_8. On day 4 postinfection, the culture supernatant was collected and the concentration of viral p24 antigen was measured by an ELISA assay. The p24 levels decreased in a dose-dependent manner with increasing the concentration of Vpr-3 R_8; 50% inhibition of p24 expression was obtained with approximately 0.8 μM of Vpr-3 R_8 (Figure 5A). This concentration was approximately 10-fold lower than the concentration of Vpr-3 R_8 known to be cytotoxic (Figure 4). Second, MT-4 cells were infected with HIV-1_{HXB2} and the replication kinetics was monitored in the presence of 0.5 μM Vpr-3 R_8. The degree of replication of HIV-1_{HXB2} was quite low in the presence of Vpr-3 R_8, while replication of HIV-1_{HXB2} was robust in the absence of Vpr-3 R_8 (Figure 5B), suggesting that Vpr-3 R_8 strongly suppresses the replication of HIV-1 in cells. To examine whether the HIV-1 replication was blocked through the inhibition of IN activity, quantitative real-time PCR was performed. If IN is inhibited, the efficiency of viral genome integration should be decreased while the reverse transcription of viral genome should not be affected. Accordingly, NP2-CD4-CXCR4 cells were infected with HIV-1_{HXB2} in the presence or absence of 0.5 μM Vpr-3 R_8. Genomic DNA was extracted on day 2 postinfection, and the viral DNA was quantified at the various steps of viral entry phase. The level of "strong stop DNA", representing the total genome of infected virus in Vpr-3 R_8-treated cells, was similar (139.7%) to that in DMSO-treated control cells and the level of viral DNA generated at the late stage of reverse transcription in Vpr-3 R_8-treated cells was slightly decreased (84.4%) compared to control cells. This small decline can probably be attributed to the weak anti-RNase H activity of Vpr-3 R_8. On the other hand, a drastic decrease of Alu-LTR products was observed in Vpr-3 R_8-treated cells (15.8%), indicating an inhibition of integrated viral genome. Concomitantly, the double LTR products, representing the end-joined viral genome catalyzed by host cellular enzymes, were increased by a factor of 8 (779.8%). These results strongly suggest that Vpr-3 R_8 blocks viral infection by inhibiting IN activity in cells, consistent with our in vitro observations. Judging by these results, Vpr-derived peptides with the R_8 group are potent IN inhibitors that suppress HIV-1 replication in vivo.

Finally, in silico molecular docking simulations of Vpr-derived peptides and HIV-1 IN were performed. The Vpr-derived peptides are located in the second helix of Vpr and were thus considered to have an α-helical conformation.[22] Docking simulations of three peptides (Vpr13, Vpr14, and Vpr15), using the predicted structure of the HIV-1 IN dimer as a template,[23] were performed by GOLD software to investigate the binding mode of the peptides, the binding affinity of